This document was prepared for the ETI by third parties under contract to the ETI. The ETI is making these documents and data available to the public to inform the debate on low carbon energy innovation and deployment.

Programme Area: Marine

Project: PerAWAT

Title: An Investigation into the effect of Ambient Turbulence Levels on the Wakes of a Conventional Low-Solidity and an Open-Centre High-Solidity Tidal Current Turbine

Abstract:

This report documents an investigation into the effect of ambient turbulence levels on the wakes of the two turbine types considered previously: a 'conventional' low-solidity turbine and an opencentre high-solidity turbine. In this sense, it can be considered an extension of the work of Deliverables One and Two. A further part of the scope of the present deliverable is to consider the necessity of updating the end-of-near-wake parameterization developed in Deliverable Three to account for the effect of the ambient turbulence. Five different intensity/length-scale combinations were investigated. For the low-solidity turbine, each of these combinations were run for five different combinations of the tip speed ratio and domain radius (i.e. domain blockage) to give a total of 25 simulations.

Context:

The Performance Assessment of Wave and Tidal Array Systems (PerAWaT) project, launched in October 2009 with £8m of ETI investment. The project delivered validated, commercial software tools capable of significantly reducing the levels of uncertainty associated with predicting the energy yield of major wave and tidal stream energy arrays. It also produced information that will help reduce commercial risk of future large scale wave and tidal array developments.

PerAWaT MA1003

An investigation into the effect of ambient turbulence levels on the wakes of a conventional low-solidity and an open-centre high-solidity tidal current turbine

WG3 WP5 D4

Dr Gareth I Gretton

The University of Edinburgh

Version: 1.0

8th March 2013

Revision history

Version	Issue date	Summary
0.1	12th November 2012	Working draft for internal (UoE) review.
0.2	14th November 2012	Working draft for internal (UoE) review.
0.3	14th November 2012	First version for review by GH and consortium.
1.0	8th March 2013	Minor revision, for submission to ETI.

Executive summary

This report documents the work done for the fourth and final deliverable of WG3 WP5 (device scale numerical modelling: detailed CFD of other concepts). Deliverable Four is an investigation into the effect of ambient turbulence levels on the wakes of the two turbine types considered previously: a 'conventional' low-solidity turbine and an open-centre high-solidity turbine. In this sense, it can be considered an extension of the work of Deliverables One and Two. A further part of the scope of the present deliverable is to consider the necessity of updating the end-of-near-wake parameterization developed in Deliverable Three to account for the effect of the ambient turbulence.

All of the CFD simulations in Deliverables One and Two used the same inlet values for the turbulence intensity and large-eddy length scale, such that the rotor-plane values were 10% and 18 m respectively. In the present work, two one-dimensional studies were conducted. In the first study, the intensity was changed to 4% and then 16% whilst keeping the large-eddy length scale constant at 18 m, while in the second study, the large-eddy length scale was changed to 9 m and then 4.5 m whilst keeping the intensity constant at 10%. Five different intensity/length-scale combinations were thus investigated. For the low-solidity turbine, each of these combinations were run for five different combinations of the tip speed ratio and domain radius (i.e. domain blockage) to give a total of 25 simulations. For the high-solidity turbine, the tip speed ratio and domain radius were not varied.

It was found that varying the turbulence properties had little effect on the power and thrust coefficient, and a minimal effect also on the velocity profiles in the immediate wake of the turbine (that is, up to about 1 diameter downstream). Further downstream, between about 2 and 4 diameters, there were more noticeable differences in the wake profiles due to the varying turbulence levels, while further downstream again the differences began to fade out. These general conclusions apply to both turbine types, and all tip speed ratio and domain radius combinations, although there were some small variations which are elaborated on in the report.

As it was concluded in Deliverable Three that the end-of-near-wake parameterization was a best fit at about 1 diameter downstream of the turbine, the current CFD results suggest that there is no requirement to make this parameterization sensitive to the levels of ambient turbulence. Instead, such differences in the far wake that are due to the varying levels of ambient turbulence should be accounted for in the far wake model.

Contents

1 Introduction to this document

Deliverable Four of WG3 WP5 (device scale numerical modelling: detailed CFD of other concepts) is an investigation into the effect of ambient turbulence levels on the performance of a tidal current turbine and the wake produced by such a turbine. As with previous work in this package, the two tidal current turbine geometries under consideration are a 'conventional' low-solidity turbine and an open-centre high-solidity turbine. The modelling methodology used in this present deliverable is that developed in Deliverables One and Two (Gretton, 2011a,b) for the low- and high-solidity turbines respectively, also as used in Deliverable Three (Gretton, 2013).[1]

These CFD models of the two turbines are based on the k-ω-SST turbulence model; chosen because it offers the optimum balance of accuracy and speed. This turbulence model consists of transport equations for two turbulence variables, k and ω; two variables which can also be written as combinations of the turbulence intensity and large-eddy length scale. It is these latter two variables which were systematically varied in the present work.

Also within the scope of the present work is the requirement to update the end-of-near-wake parameterization developed in Deliverable Three to include a sensitivity to the ambient turbulence levels, as necessary. Some of the existing end-of-near-wake parameterizations for wind turbine wakes include such a sensitivity while others do not, and where present in these existing models the sensitivity is normally weak (see the D3 report for details). It was thus not clear at the outset whether such a sensitivity is required, and in one sense answering this question is the key conclusion of the present work.

The initial acceptance criteria for this deliverable included the objectives noted above, and also an investigation into the effect of an upstream device on a downstream device. As specified in Variation Request 34, this secondary investigation was removed from the acceptance criteria owing to severe time pressures, and following consultation with GL Garrad Hassan on which was the most useful output from the perspective of the 'end user'.

Regarding dependencies and linkages, the present deliverable is a dependency of WG3 WP4 D15 and was required before the 18th of January 2013, hence the narrowing of objectives already

[1] These are henceforth referred to as the 'D1', 'D2' and 'D3' reports.

noted. As will be seen from the revision history, this document was originally delivered ahead of this deadline, with only minor editorial amendments made later.

2 Modelling overview

The CFD work in the present deliverable utilizes the models developed for the low- and high-solidity turbines in Deliverables One and Two respectively, and the reader is referred to these reports for details of the models. To summarize here, both of the models are Reynolds-Averaged Navier-Stokes (RANS) solutions, based on the absolute-velocity rotating frame of reference approach. The computational grid fully resolves the true turbine geometry, including full resolution of the boundary layer on the blades. This may be referred to as a 'blade-resolved' simulation, and does *not* involve the use of an actuator-disc approximation.

Given the rotating frame of reference approach, only a single blade of each of the turbines is considered. This means that for the low-solidity turbine the domain extends through 120° while that for the high-solidity turbine extends through 22.5°. Axially, the domains extend 5 turbine or duct diameters (as applicable) upstream and 40 diameters downstream. The standard radial extent is 4 turbine or duct radii, but domains extending to 2 and 8 turbine radii are also used for the low-solidity turbine to investigate the effect of blockage.

The k-ω-SST turbulence model is used throughout this work, as it is believed to offer the optimum balance of accuracy and speed for the present modelling objectives. Two turbulence variables are modelled with this: the turbulence kinetic energy, k, and the dissipation per unit turbulence kinetic energy, ω, sometimes also called the turbulence frequency due to its units. These variables are somewhat abstract but can be calculated based on any two alternative measures of the state of turbulence having different dimensions, and we use here the turbulence intensity, Ti, and the large-eddy length scale, ℓ:

$$k = \frac{3}{2}(U_{\text{ref}} Ti)^2 \tag{1}$$

$$\omega = \sqrt{k}/(C_\mu \ell) \tag{2}$$

where U_{ref} is taken as the inlet velocity, and C_μ is a constant, normally 0.09. Whilst the relation between k and Ti is near-universal, alternative definitions for the relation between ω, k and ℓ, do exist, as the definition of the large-eddy length scale can vary; the relations shown here are taken from Versteeg and Malalasekera (2007). Care must therefore be taken when comparing reported values for the large-eddy length scale. Also note that 'LLE' (Length-Large-Eddy) is used in this report to represent the large-eddy length scale, and is equivalent to ℓ.

In the modelling work done for Deliverables One and Two, the inlet values of these variables were chosen such that the values at the rotor plane were 10% and 18 m respectively. Inlet values and values at the rotor plane are different because there is decay of turbulence between these two locations, leading to a drop in the turbulence intensity and an increase in the large-eddy length scale.[2] In the present work, different *rotor plane* intensities and length scales were targeted as follows: for a turbulence intensity of 4%, length scales of 4.5 m, 9 m and 18 m have been specified, while for a length scale of 18 m, turbulence intensities of 4% (as before), 10% and 16% have been specified. The missing combinations are not possible to achieve due to dissipation between the inlet and the rotor plane. Inlet values for the intensity and length scale which lead (in the absence of shear) to the desired rotor plane values are given in Table 1.

Table 1: *Inlet values for the turbulence intensity/large-eddy length scale.*

	LLE (m)		
Ti (%)	4.5	9	18
4	14.1/1.6	5.5/6.8	4.6/16.0
10	–	–	15.7/12.3
16	–	–	56.3/6.3

These ranges for the turbulence intensity and length scale are intended to span the range of realistic values for tidal turbine deployment sites. Numerous studies have been conducted with a variety of instrumentation to determine these values, with a significant amount of variation in the reported values. Some of this variation will of course be due to the differing sites, but it is felt by the present author that a significant amount of variation may also be due to the instrumentation used and the method of processing the raw data; there is thus some uncertainty as to the 'true' values of these variables at deployment sites. As an example of a recent paper

[2]The large-eddy length scale increases, despite the overall decay of turbulence, because the smaller eddies decay more rapidly than the larger eddies. This is explained in greater depth in Pope (2008).

reporting intensity and length scale measurements towards the upper-middle of the range of values used here, see Milne et al. (2011).

It might also be noted here that as the k-ω-SST turbulence model is an *eddy-viscosity* model, the impact of turbulence on the momentum equation is through the single variable of the eddy viscosity, which may be calculated from k and ω or Ti and ℓ as:

$$\nu_{\text{turb}} = k/\omega \tag{3}$$

$$= \sqrt{\frac{3}{2}}\, C_\mu\, U_{\text{ref}}\, Ti\, \ell \tag{4}$$

Thus, the eddy-viscosity is linearly dependent on both the turbulence intensity and the length scale i.e. flows with larger length scales are more turbulent (as of course are flows with higher intensities).

Simulation parameters which were varied in previous studies were the tip speed ratio and the blockage ratio (although the latter was only varied in the study of the low-solidity turbine). In the present work, these parameters were again varied for each of the turbulence intensity/length scale combinations noted above. For the low-solidity turbine the test matrix of tip speed ratio and blockage ratio is shown in Table 2, while for the high-solidity turbine only a single tip speed ratio/blockage ratio combination was used: namely, TSR = 2.8 and the mesh extending to 4 duct radii in the radial direction.

Table 2: *Tip speed ratio/domain radius test matrix. R_t is the turbine radius.*

	Domain radius		
TSR	$2R_t$	$4R_t$	$8R_t$
3		✔	
5	✔	✔	✔
7		✔	

3 Results and discussion

All of the results produced by the simulations outlined above are contained in Appendices B and C, the former containing tables of the power and thrust coefficients, and the latter containing figures showing longitudinal and lateral profiles of the velocity and pressure. Furthermore, an explanation of the layout of the data is provided in Appendix A. We thus here proceed immediately to a discussion of these results.

Considering first the results for the power and thrust coefficients, for the low-solidity turbine, and for the domain extending to 4 turbine radii, only small changes are observed with changing levels of turbulence (Tables 4–6). These changes are generally less than or around 1% relative to the 10% intensity/18 m length-scale case. Larger changes – up to 7% – are seen for the power coefficient and for the higher turbulence case. Also, it is seen that variation in the length-scale has almost no effect. For the simulations on the 2 turbine radii domain the pattern is generally similar to the above (Table 7), but for the 8 turbine radii domain there are much larger differences between the simulations, especially for the thrust coefficient (Table 8). Given the lack of pattern, and given that this is not consistent with any of the other results, this must be viewed with suspicion. Unfortunately there was insufficient time to rigorously interrogate these results and so they are issued here with a caution regarding their veracity.

For the high-solidity turbine there is slightly more variation with the turbulence levels (excluding those from the $8R_t$ mesh) – approximately ±7% – and especially for the thrust coefficient (Table 9). Specifically, there is a more significant change from the reference case to the low turbulence cases. It is also observed that there is an increase in the power and thrust coefficients with increasing turbulence levels – the opposite of the trend observed for the power coefficient on the low-solidity turbine.

Turning to the velocity and pressure profiles (Figures 1–24), it may first be noted that pressure profiles have not previously been included in the results presented in Deliverables One to Three. They are included here primarily because it is thought they may be useful in future work. The pressure profiles also show two key aspects of the solution: First, the classical pattern of pressure rise ahead of the turbine, followed by rapid pressure drop through the rotor plane, and subsequent recovery. As one of the ‘definitions’ of the end-of-near-wake region is that static pressure recovery has occurred (or mostly occurred) these results provide data to determine the

location of this region. Second, we can observe that there is a net pressure drop from the inlet to the outlet, that is a function of the blockage ratio and the tip speed ratio/thrust coefficient, and with higher blockage ratios and higher thrust coefficients producing a greater pressure drop. This is a feature of a turbine operating in a blocked environment, and would not be observed in the case of a wind turbine.

With regards to the effect of turbulence on the velocity profiles, these are normally small, especially in the immediate wake (that is up to about 1 diameter downstream). Further, and as with the power and thrust coefficients, the effect of varying the large-eddy length scale is negligible, while the most significant effect is a result of changing the intensity from 10% to 16% (as opposed to 4% to 10%). These effects are common across all of the tip speed ratio/blockage ratio combinations investigated, and for both the low- and high-solidity turbines. It might also be noted that the effect of varying the turbulence intensity is as would be expected: higher levels of turbulence lead to greater mixing and therefore more rapid wake recovery.

As a final observation on the profiles, certainly the most visible change in either the velocity or the pressure with turbulence levels occurs for the pressure on the most highly-blocked cases (Figure 16). This is most probably a direct result of the fact that the largest pressure changes from inlet to outlet occur for this case. The effect of changes in turbulence intensity is such that higher values lead to a greater pressure drop through the domain, this most likely resulting from greater mixing. Confusingly though, larger values of the large-eddy length scale lead to a smaller pressure drop. Irrespective of this, the variation in the velocity field is minimal.

4 Conclusions

Two straightforward conclusions may be offered from the present set of results: First, variation in the levels of ambient turbulence has little effect on the power and thrust coefficient, and a minimal effect also on the velocity profiles in the immediate wake (that is up to about 1 diameter downstream). This is especially so for variation of the large-eddy length scale which has negligible effect. This in turn means that the end-of-near-wake parameterization developed in Deliverable Three does not need to be updated, as it was concluded there that this fitted best at around 1 diameter downstream.

Second, the differences that are observed in the wake velocity profiles with varying levels of the ambient turbulence intensity occur further downstream (at and after about 2 diameters), and become more significant progressing downstream (up to around 4 diameters) before beginning to fade out. Such differences should be accounted for by a far-wake model which is sensitive to turbulence, as is indeed the case with GL Garrad Hassan's existing WindFarmer software.

A Summary of the data in the appendix

The following two appendix sections consist of tables and figures presenting all of the data generated by the CFD simulations carried out for the present deliverable. Each table, and each set of four figures, contains the data for the five turbulence intensity/length scale simulations run for each combination of the tip speed ratio/domain radius.

As stated in the body of the report, the five different combinations for the turbulence intensity/large-eddy length scale are as follows: for a turbulence intensity of 4%, length scales of 4.5 m, 9 m and 18 m are considered, while for a length scale of 18 m, turbulence intensities of 4% (as before), 10% and 16% are considered. See the left-hand side of Table 3 for a summary of this. Note also that these combinations are shown in a legend once on each of the pages of figures but are consistent throughout.

For the low-solidity turbine, both the tip speed ratio and the domain radius (and hence blockage ratio) have been systematically varied in separate 1-D studies (and for each point of which the turbulence intensity and length scale have been varied as above). This involves simulations with tip speed ratios of 3.0, 5.0 and 7.0 on a mesh extending to 4 turbine radii in the radial direction, and simulations on meshes extending to 2, 4 (as before) and 8 turbine radii for a tip speed ratio of 5.0. See the right-hand side of Table 3 for a summary of this.

Table 3: *Turbulence intensity/large-eddy length scale test matrix (left) and tip speed ratio/domain radius test matrix for the low-solidity turbine (right). Each tick in the table at right can be though of as consisting of the entire table at left (or vice-versa).* R_t *is the turbine radius.*

	LLE (m)		
Ti (%)	4.5	9	18
4	✔	✔	✔
10			✔
16			✔

	Domain radius		
TSR	$2R_t$	$4R_t$	$8R_t$
3		✔	
5	✔	✔	✔
7		✔	

For the open-centre, high-solidity turbine, only a single tip speed ratio/domain radius case was considered, namely, a tip speed ratio of 2.8 and a domain radius of 4 *duct* radii.

All of the above permutations add up to a total of 25 individual simulations for the low-solidity turbine and 5 individual simulations for the high-solidity turbine. Each simulation of the low-

solidity turbine took approximately 12 hours of wall-clock time on 48 processors, while the high-solidity simulations took approximately 36 hours, again on 48 processors. This totals just over 23k CPU hours, or approximately 2.6 CPU years.

Returning to the content of the data, the tables (Appendix B) list power and thrust coefficients for every simulation, grouped according to a given tip speed ratio/domain radius combination. In each table, percentage differences are calculated for the power and thrust coefficients, relative to the case of a turbulence intensity of 10% and a large-eddy length scale of 18 m (this being the combination used in D1 and D2). This gives a quick assessment of the importance of the ambient turbulence levels in each group of cases.

The figures of Appendix C are arranged in a standard format and show the effect on the wake of varying levels of inlet turbulence for both types of turbine and under a number of different operating conditions.

Longitudinal and lateral profiles are given for both the normalized velocity and the pressure coefficient, with each combination of the above (longitudinal/lateral and velocity/pressure) occupying a single page. Furthermore, profiles are given for a number of different locations.

In presenting all of the data discussed above, it has been the aim to use as consistent a format as possible, which extends to the data ranges used for the graphs. In all cases the ranges of the coordinate variable are constant, but the range of the velocity or pressure varies somewhat, as outlined below:

- For the longitudinal velocity profiles, the velocity range is constant across all of the low-solidity turbine simulations, but different for the high-solidity turbine simulations.
- For the longitudinal pressure profiles, the pressure range is constant throughout.
- For the lateral velocity profiles the pattern is as with the longitudinal velocity profiles: constant for the low-solidity turbine simulations, but different for the high-solidity turbine simulation.
- For the lateral pressure profiles, the pattern is somewhat more complicated. For all of the low- and high-solidity turbine simulations except the low-solidity case on the 2 turbine radii mesh, there is a constant range for all of the profiles except that at $x/D = -0.5$. This uses a different range (but the same scale) which is constant across all cases. For the

simulations on the 2 turbine radii mesh, different ranges are used for both the $x/D = -0.5$ and $x/D = 0.0$ profiles, but the scale is again constant.

Regarding the pressure normalization, it should be noted that the location at which the reference pressure is taken varies slightly between the simulations. For all of the simulations of the low-solidity turbine on the meshes extending to 2 and 4 turbine radii, the reference point is at the maximum axial and radial extent, and at $z = 0$ i.e., on the outlet plane and at the perimeter of the domain. For the low-solidity simulation on the mesh extending to 8 turbine radii, this reference point was moved to 16 diameters downstream of the rotor plane (and hence 24 diameters upstream of the outlet plane). This was necessitated because of the existence of small pressure oscillations towards the outlet which would have confused the presentation of results.

For the high-solidity turbine simulations, the reference point was also moved to 16 diameters downstream of the rotor plane, in this case because the simulations had not fully converged in the (very) far-wake. This was discussed in the D2 report, where it was demonstrated that this lack of complete convergence in the far-wake does not influence the solution further upstream, which is where it is of interest in the current work.

Finally, it should be emphasized that if all of the computational domains only extended to 16 diameters downstream of the rotor plane, and this was the reference location, the results for the pressure would be equivalent to those from the present work where the reference location is 16 diameters downstream. The reason not to take the reference point at this location for some of the results is because it would hide a small aspect of the solution in the (very) far-field, namely the pressure changes which occur there.

B Tables of power and thrust coefficients

Table 4: *Low-solidity turbine,* $R_d = 4R_t$, $\lambda = 5.0$

Ti (%)/LLE (m)	C_P	C_P (%)	C_T	C_T (%)
4/4.5	0.574	0.85	0.974	−0.72
4/9	0.573	0.82	0.974	−0.64
4/18	0.574	1.01	0.975	−0.57
10/18	0.569	–	0.981	–
16/18	0.539	−5.18	0.974	−0.64

Table 5: *Low-solidity turbine,* $R_d = 4R_t$, $\lambda = 3.0$

Ti (%)/LLE (m)	C_P	C_P (%)	C_T	C_T (%)
4/4.5	0.462	0.65	0.744	−0.42
4/9	0.462	0.68	0.744	−0.43
4/18	0.463	0.82	0.744	−0.35
10/18	0.459	–	0.747	–
16/18	0.432	−5.84	0.730	−2.21

Table 6: *Low-solidity turbine,* $R_d = 4R_t$, $\lambda = 7.0$

Ti (%)/LLE (m)	C_P	C_P (%)	C_T	C_T (%)
4/4.5	0.569	0.19	1.090	−1.33
4/9	0.569	0.22	1.089	−1.38
4/18	0.572	0.71	1.093	−0.99
10/18	0.568	–	1.104	–
16/18	0.527	−7.07	1.103	−0.14

Table 7: *Low-solidity turbine,* $R_d = 2R_t$, $\lambda = 5.0$

Ti (%)/LLE (m)	C_P	C_P (%)	C_T	C_T (%)
4/4.5	0.692	−0.61	1.090	−1.52
4/9	0.695	−0.17	1.091	−1.43
4/18	0.699	0.34	1.095	−1.04
10/18	0.696	–	1.107	–
16/18	0.669	−3.88	1.101	−0.52

Table 8: *Low-solidity turbine,* $R_d = 8R_t$, $\lambda = 5.0$

Ti (%)/LLE (m)	C_P	C_P (%)	C_T	C_T (%)
4/4.5	0.547	1.03	1.153	23.47
4/9	0.546	0.86	0.625	−33.15
4/18	0.548	1.15	0.672	−28.03
10/18	0.541	–	0.934	–
16/18	0.513	−5.22	1.094	17.10

Table 9: *High-solidity turbine,* $R_d = 4R_t$, $\lambda = 2.8$

Ti (%)/LLE (m)	C_P	C_P (%)	C_T	C_T (%)
4/4.5	0.247	−6.42	0.389	−5.86
4/9	0.249	−5.79	0.391	−5.41
4/18	0.250	−5.28	0.392	−5.03
10/18	0.264	–	0.413	–
16/18	0.280	6.00	0.444	7.53

C Figures showing velocity and pressure profiles

Low-solidity turbine, $R_d = 4R_t$**,** $\lambda = 5.0$

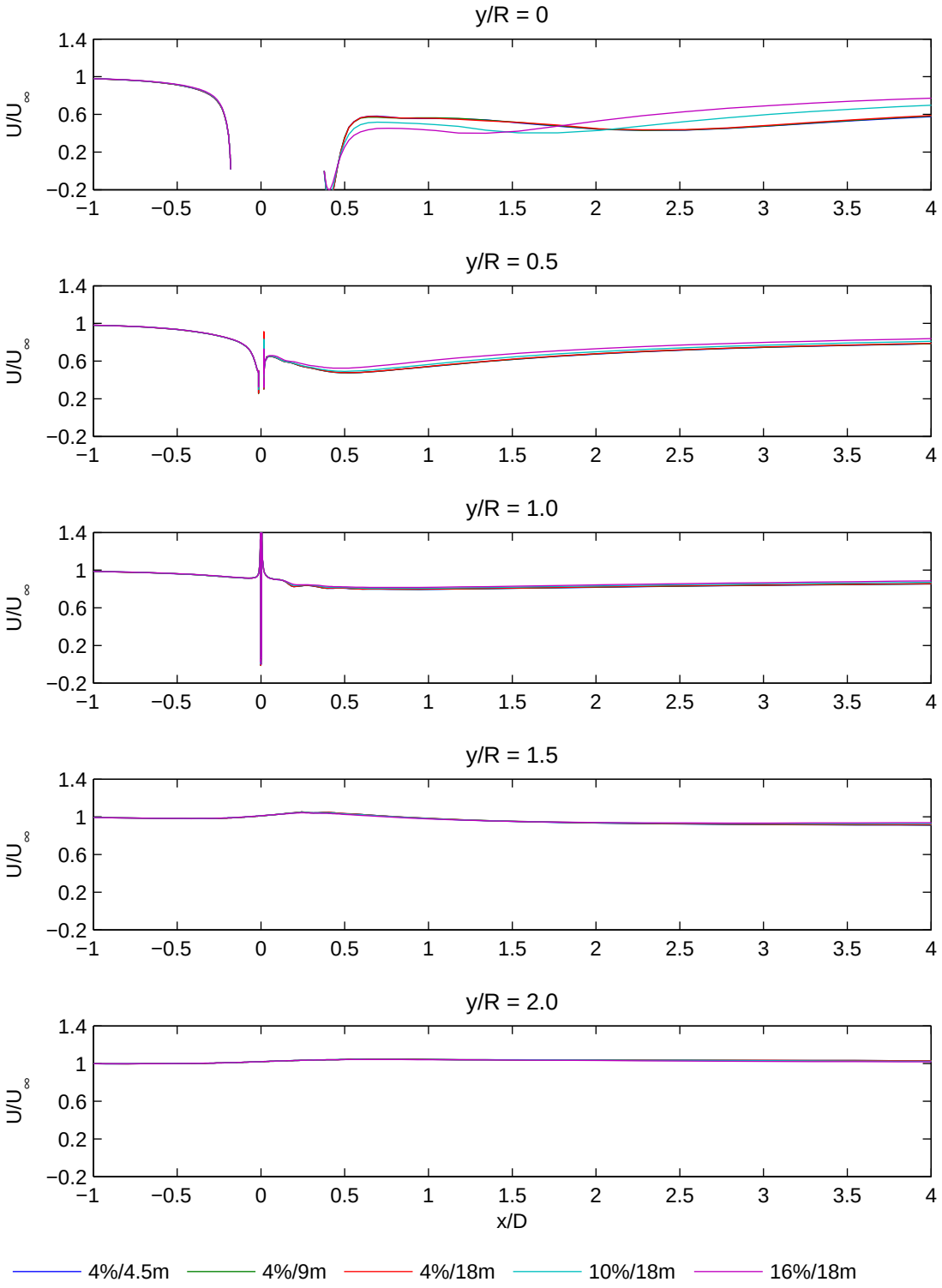

Figure 1: *Longitudinal velocity profiles.*

. . . low-solidity turbine, $R_d = 4R_t$, $\lambda = 5.0$ . . .

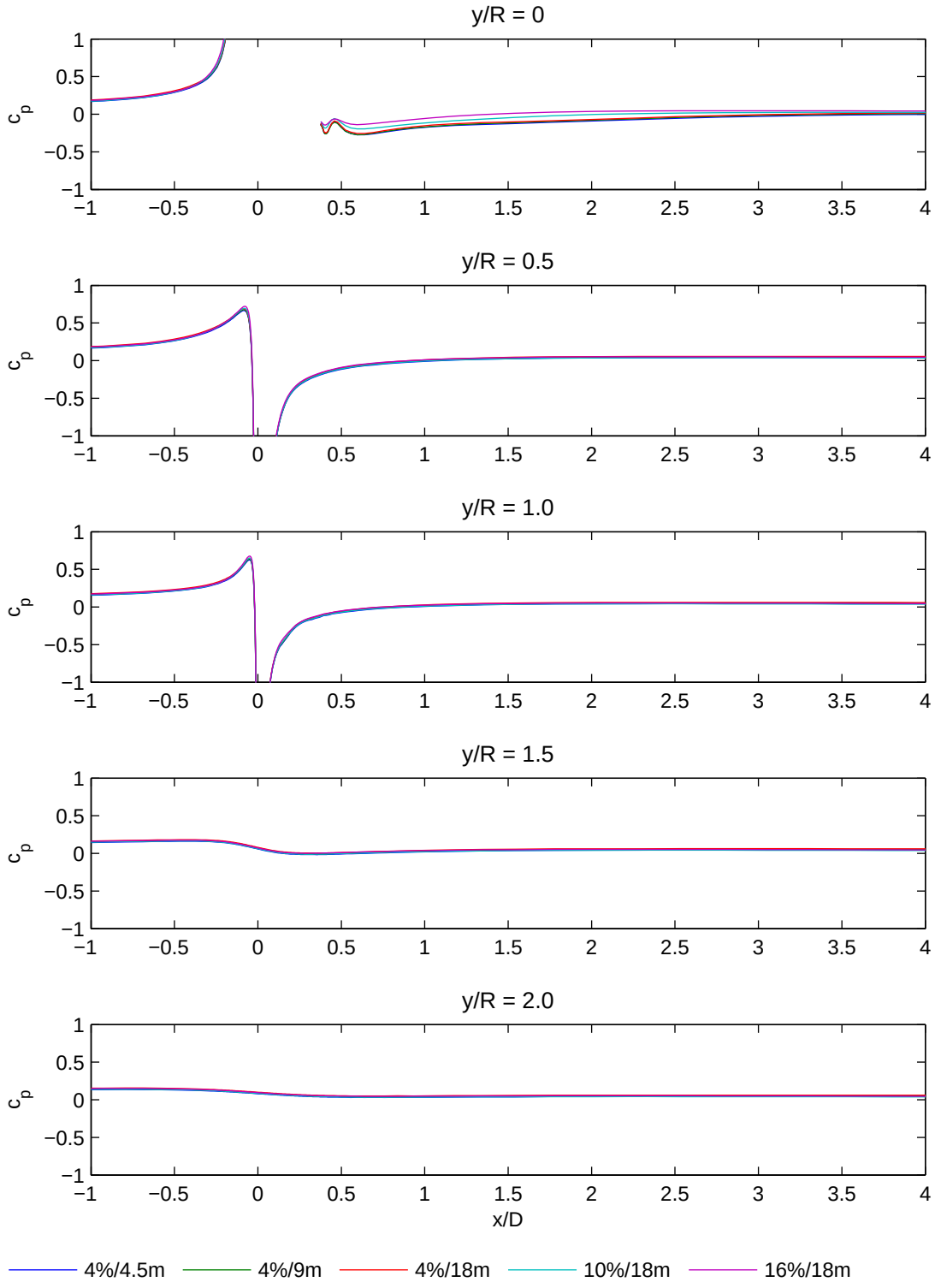

Figure 2: *Longitudinal pressure profiles.*

. . . low-solidity turbine, $R_d = 4R_t$, $\lambda = 5.0$ . . .

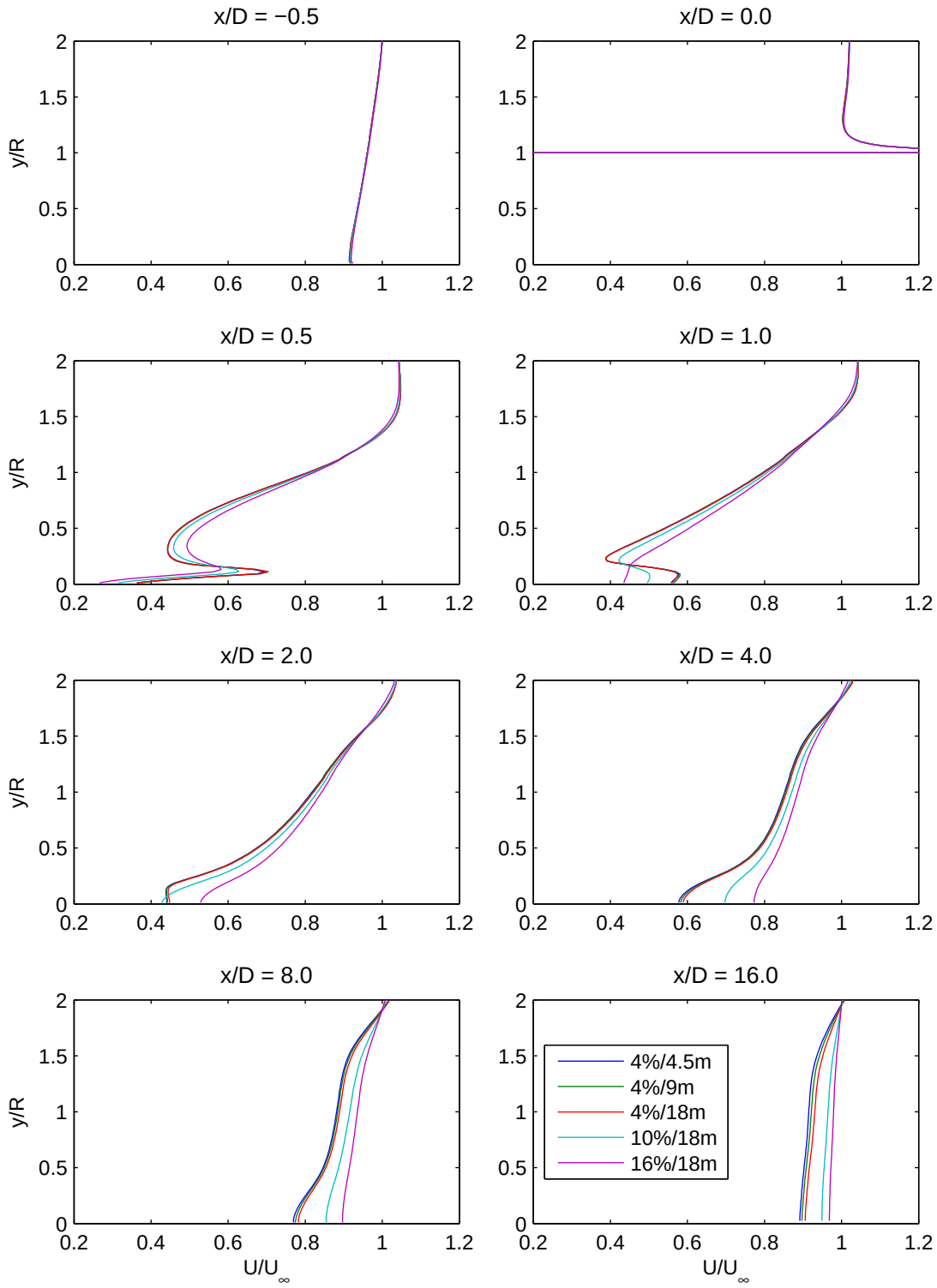

Figure 3: *Lateral velocity profiles.*

... low-solidity turbine, $R_d = 4R_t$, $\lambda = 5.0$

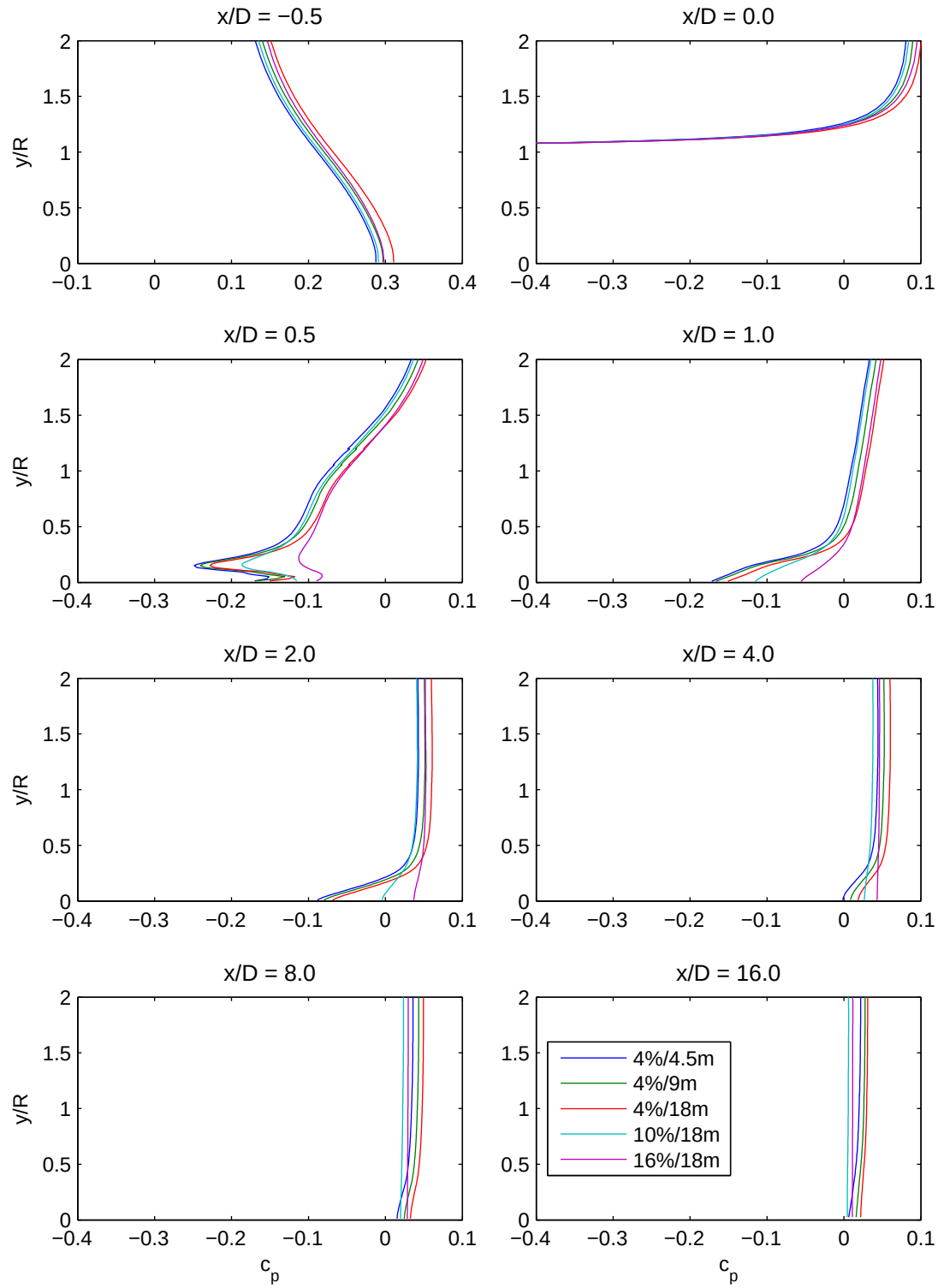

Figure 4: *Lateral pressure profiles.*

Low-solidity turbine, $R_d = 4R_t$**,** $\lambda = 3.0$

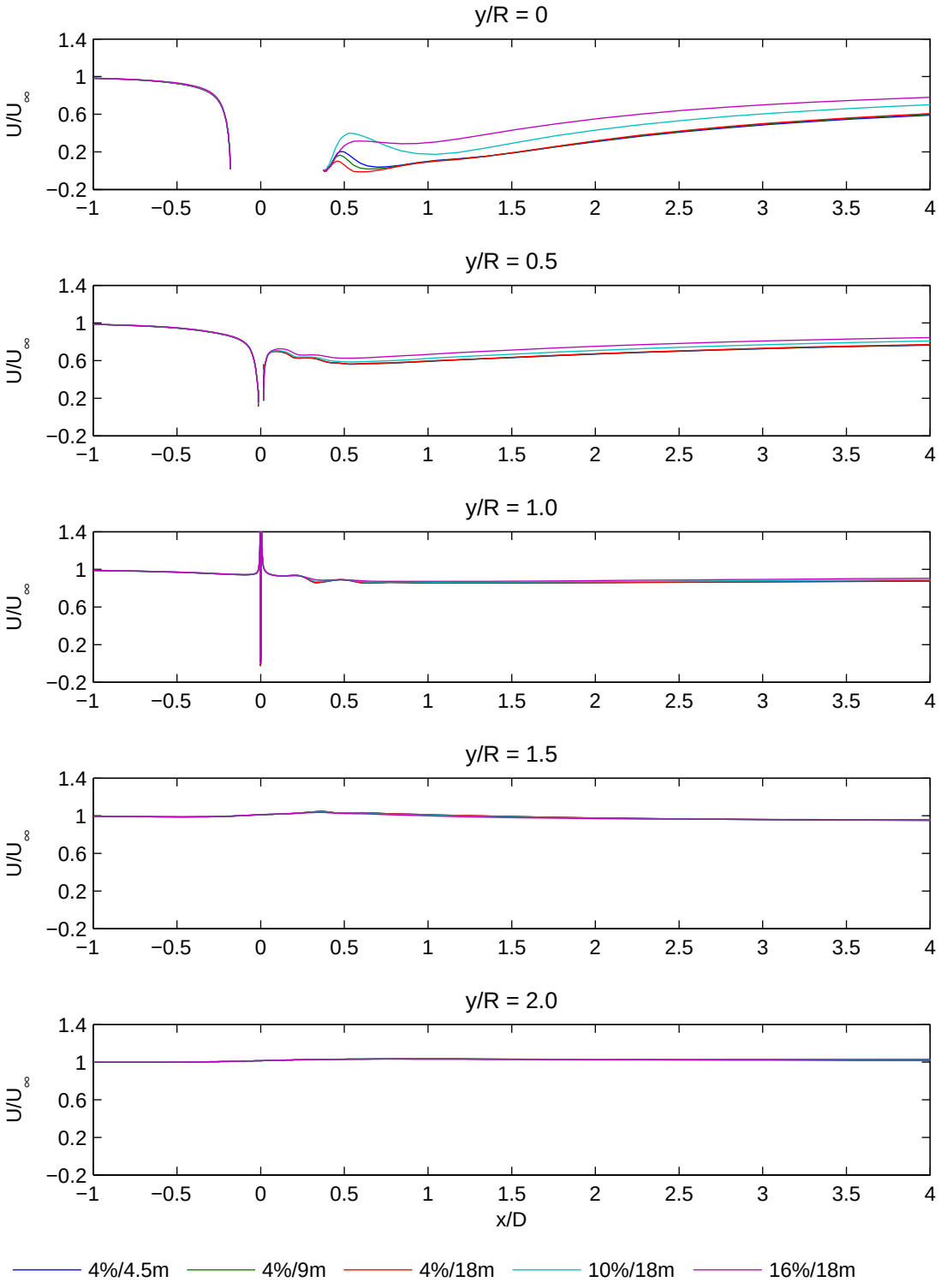

Figure 5: *Longitudinal velocity profiles.*

. . . low-solidity turbine, $R_d = 4R_t$, $\lambda = 3.0$ . . .

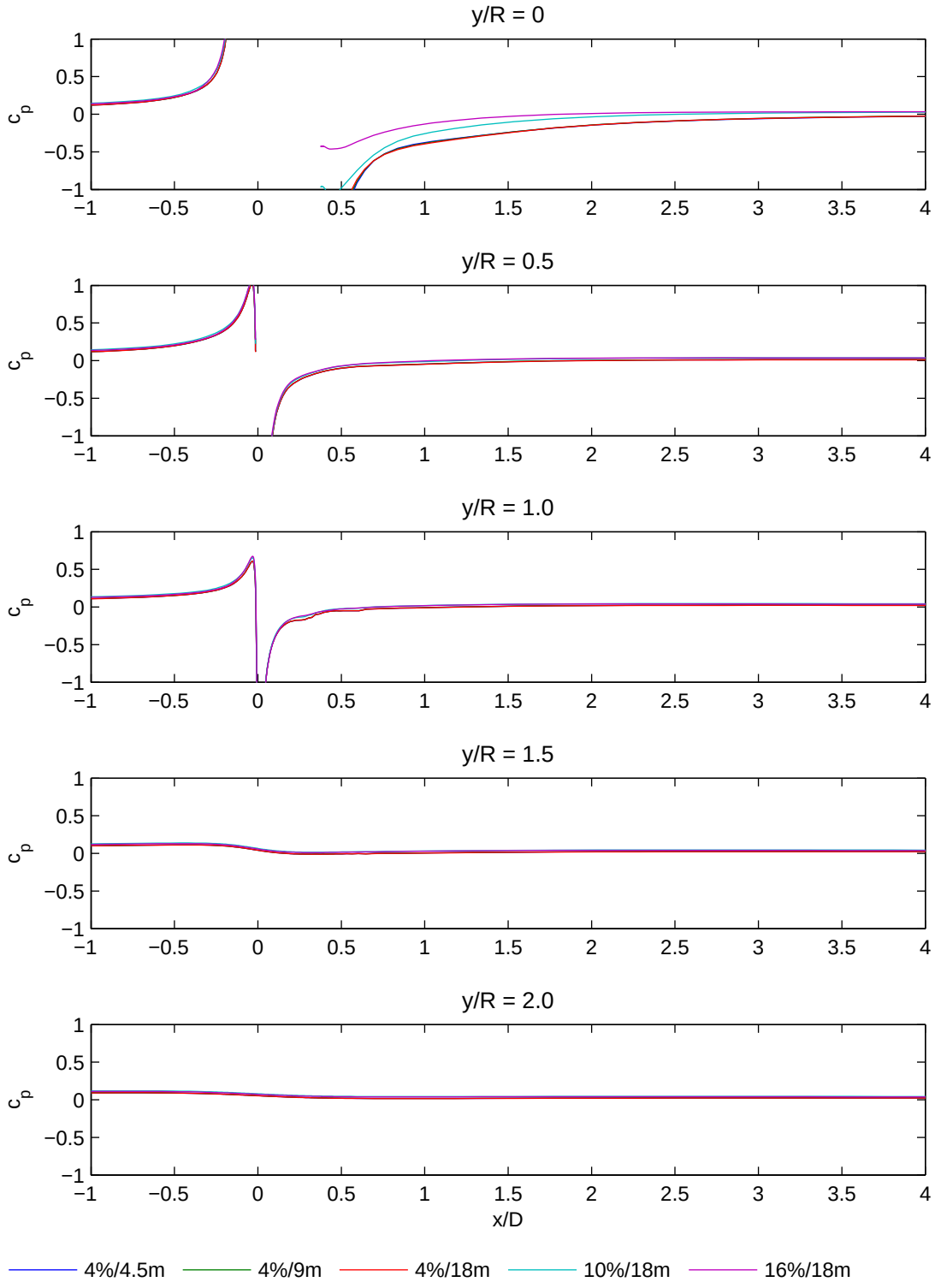

Figure 6: *Longitudinal pressure profiles.*

... low-solidity turbine, $R_d = 4R_t$, $\lambda = 3.0$ ...

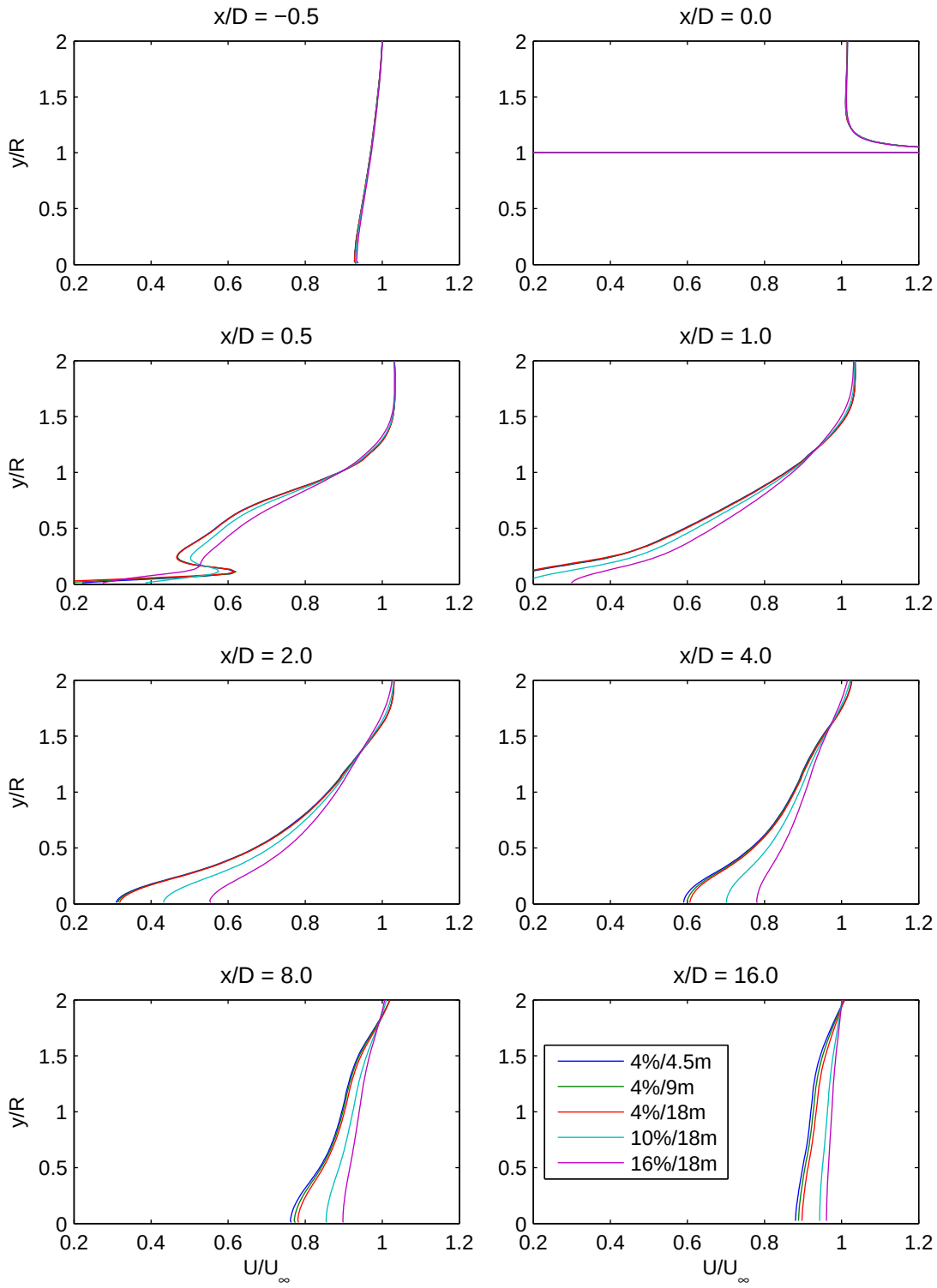

Figure 7: *Lateral velocity profiles.*

... low-solidity turbine, $R_d = 4R_t$, $\lambda = 3.0$

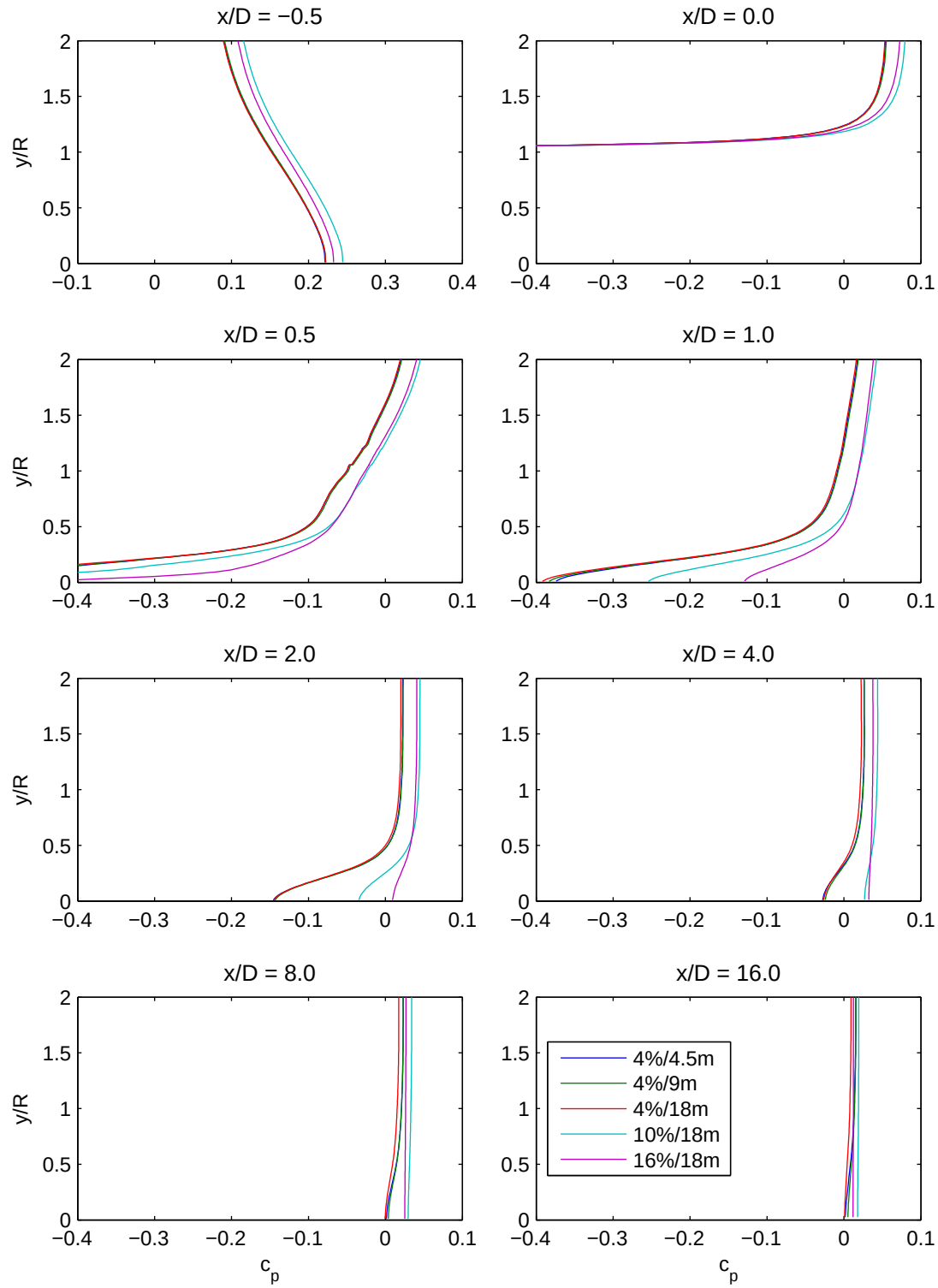

Figure 8: *Lateral pressure profiles.*

Low-solidity turbine, $R_d = 4R_t$**,** $\lambda = 7.0$

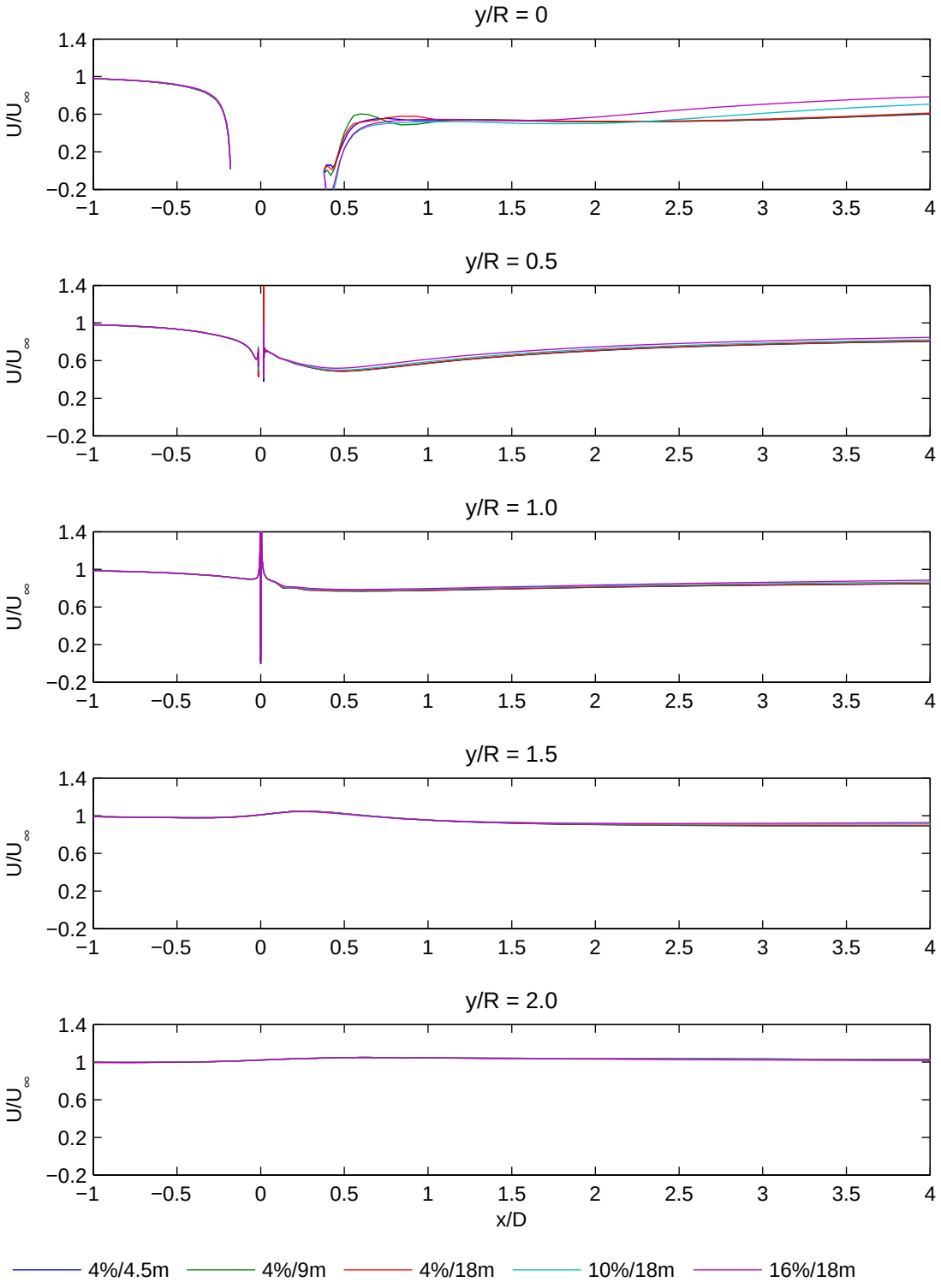

Figure 9: *Longitudinal velocity profiles.*

. . . low-solidity turbine, $R_d = 4R_t$, $\lambda = 7.0$ . . .

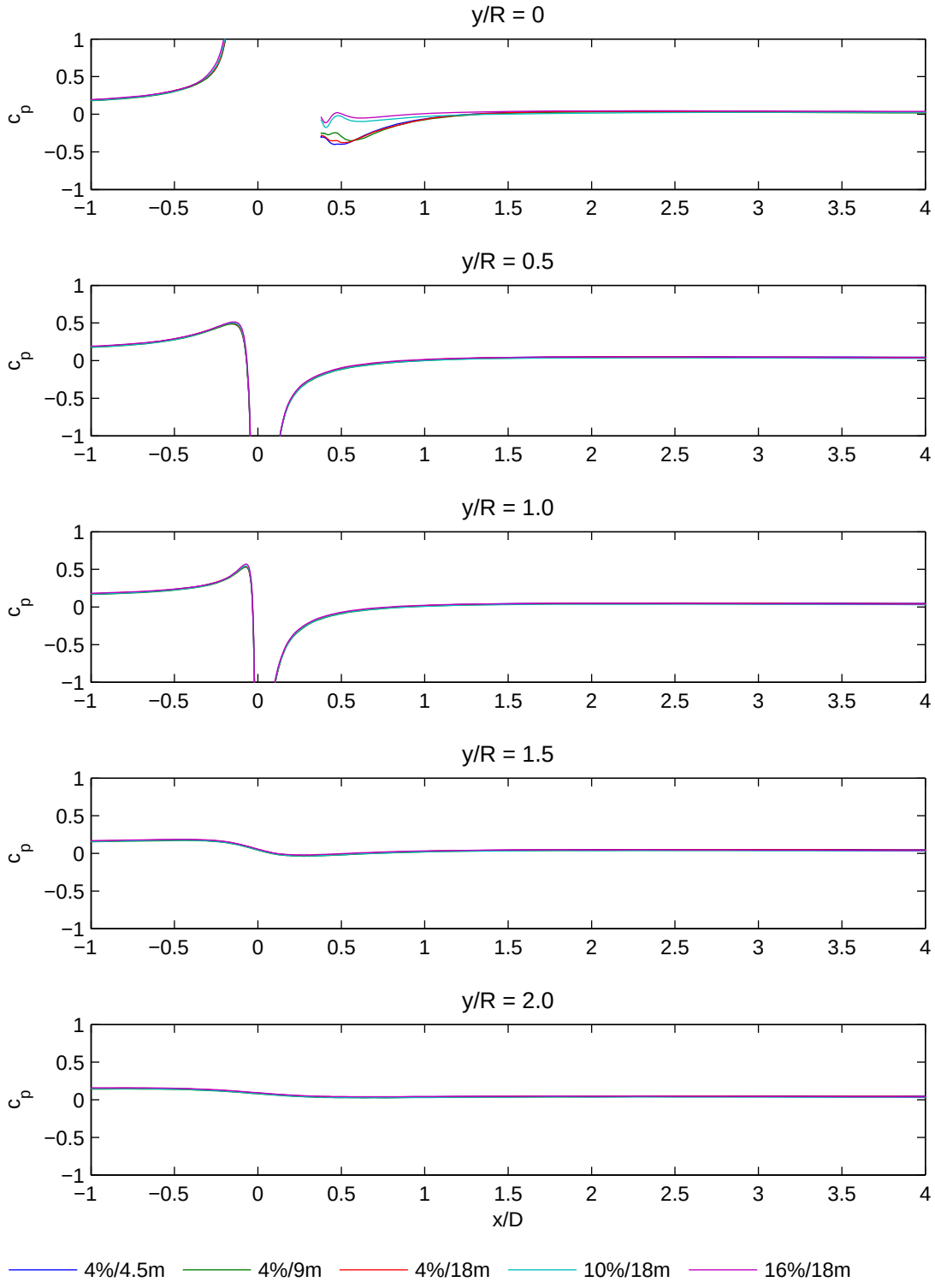

Figure 10: *Longitudinal pressure profiles.*

. . . low-solidity turbine, $R_d = 4R_t$, $\lambda = 7.0$ . . .

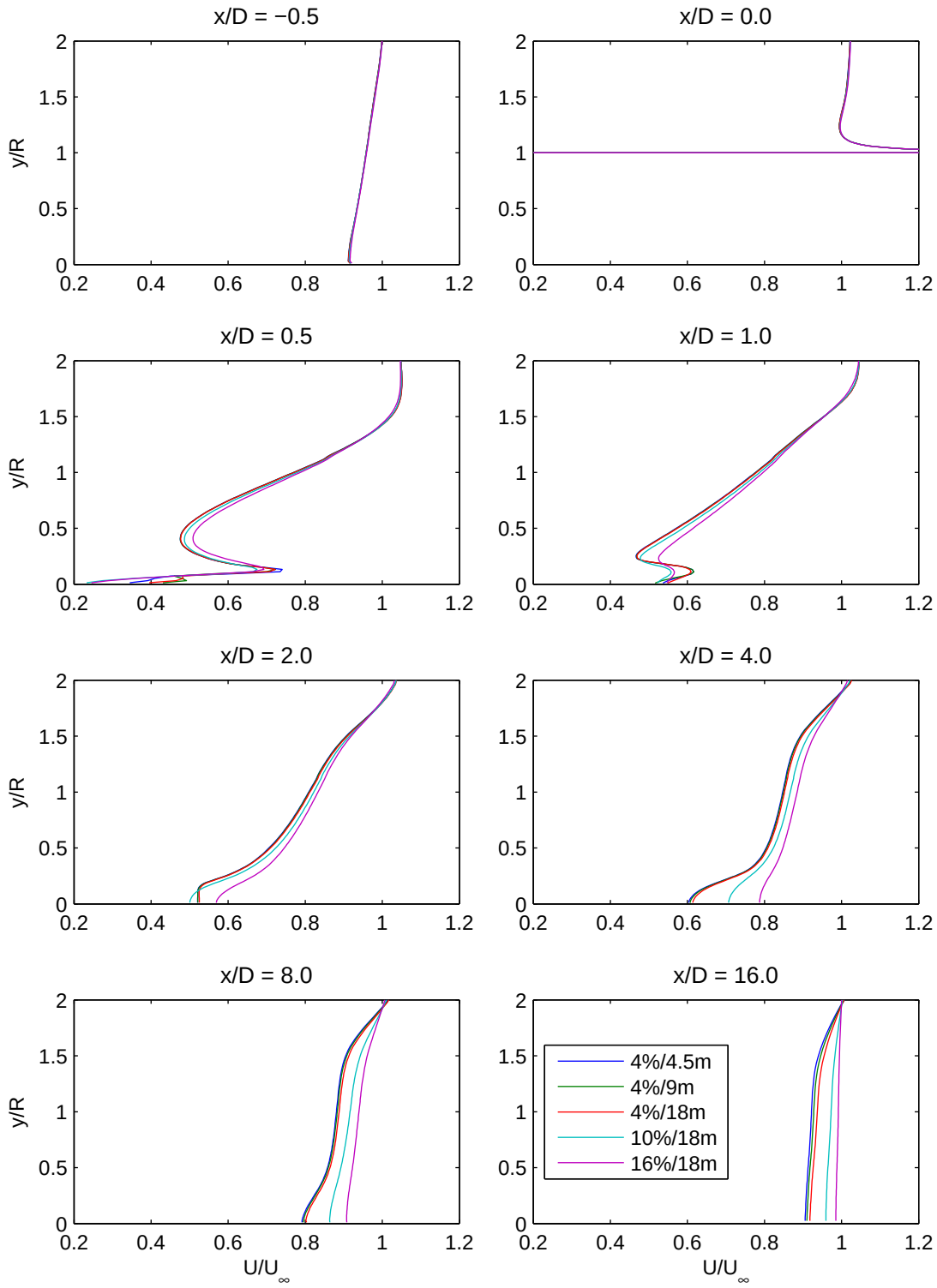

Figure 11: *Lateral velocity profiles.*

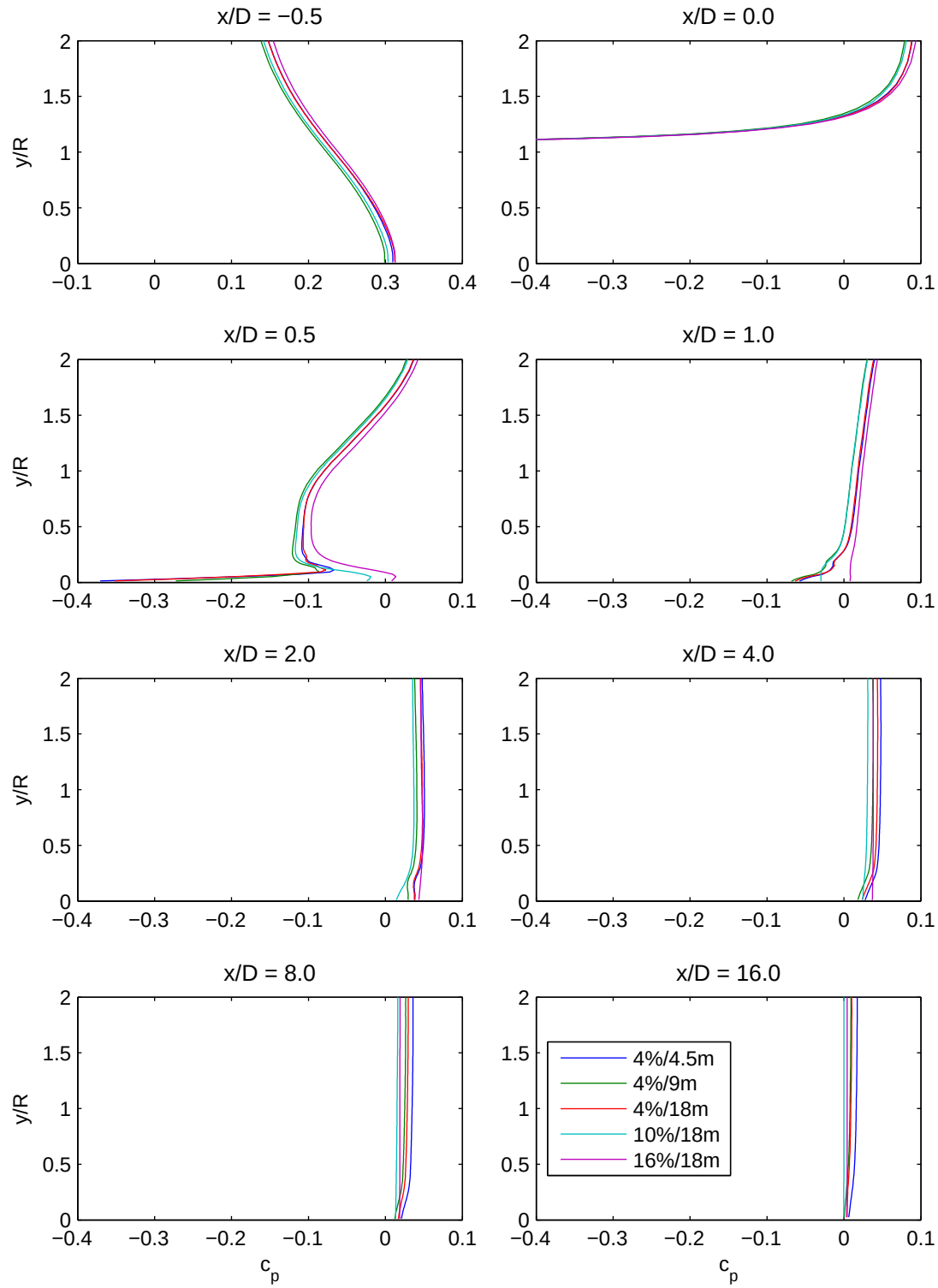

Figure 12: *Lateral pressure profiles.*

Low-solidity turbine, $R_d = 2R_t$**,** $\lambda = 5.0$

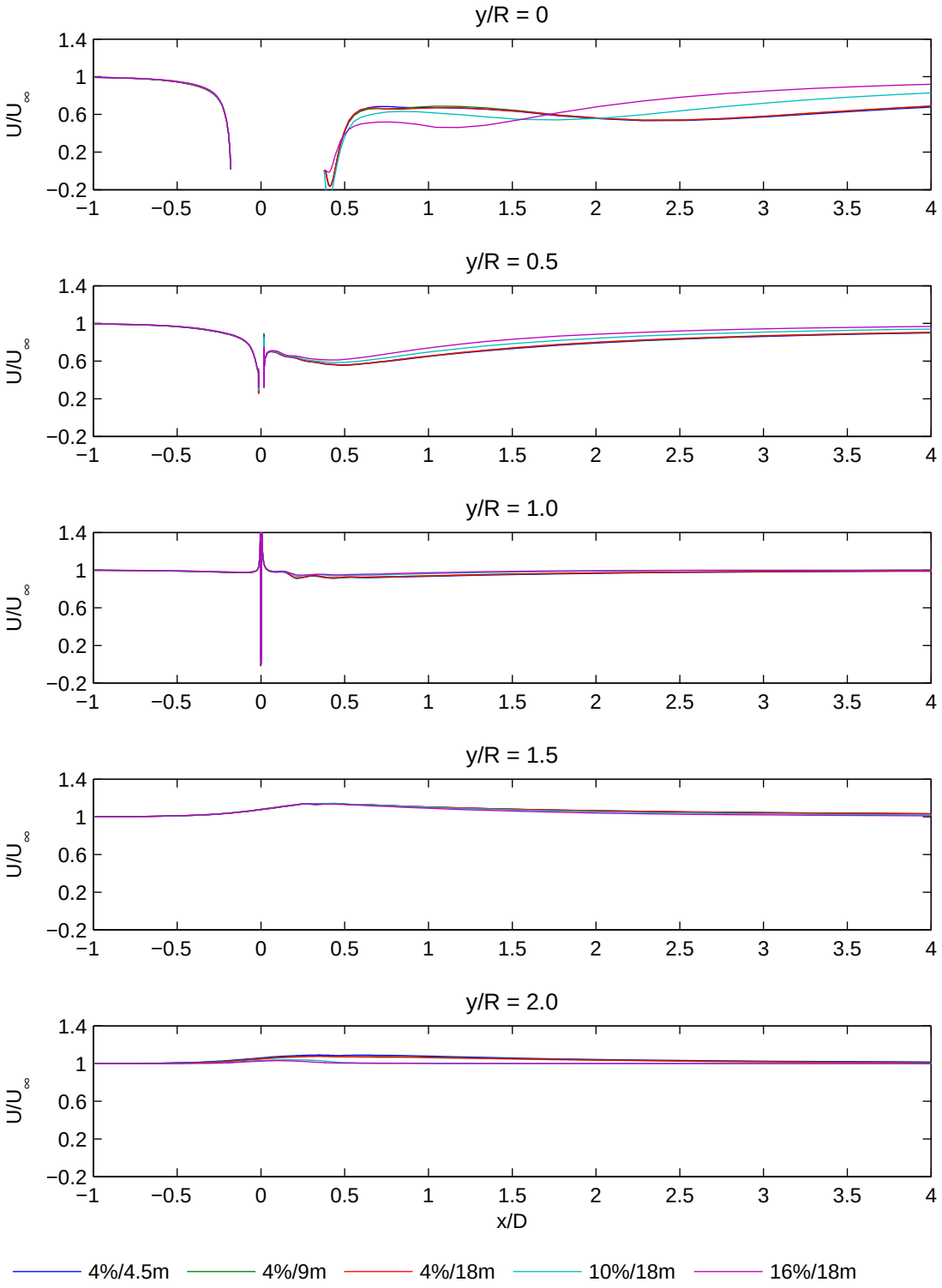

Figure 13: *Longitudinal velocity profiles.*

. . . low-solidity turbine, $R_d = 2R_t$, $\lambda = 5.0$ . . .

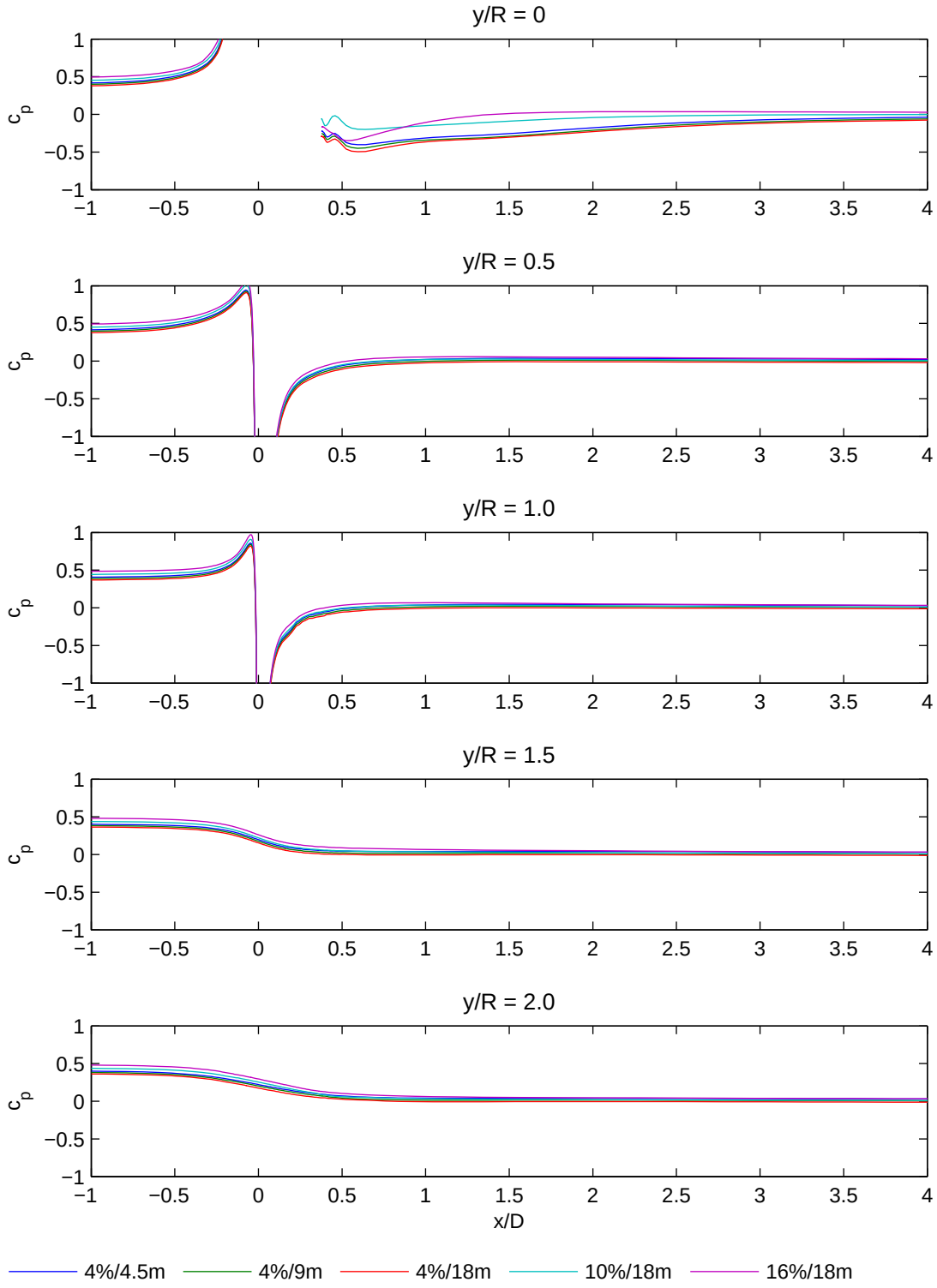

Figure 14: *Longitudinal pressure profiles.*

. . . low-solidity turbine, $R_d = 2R_t$, $\lambda = 5.0$ . . .

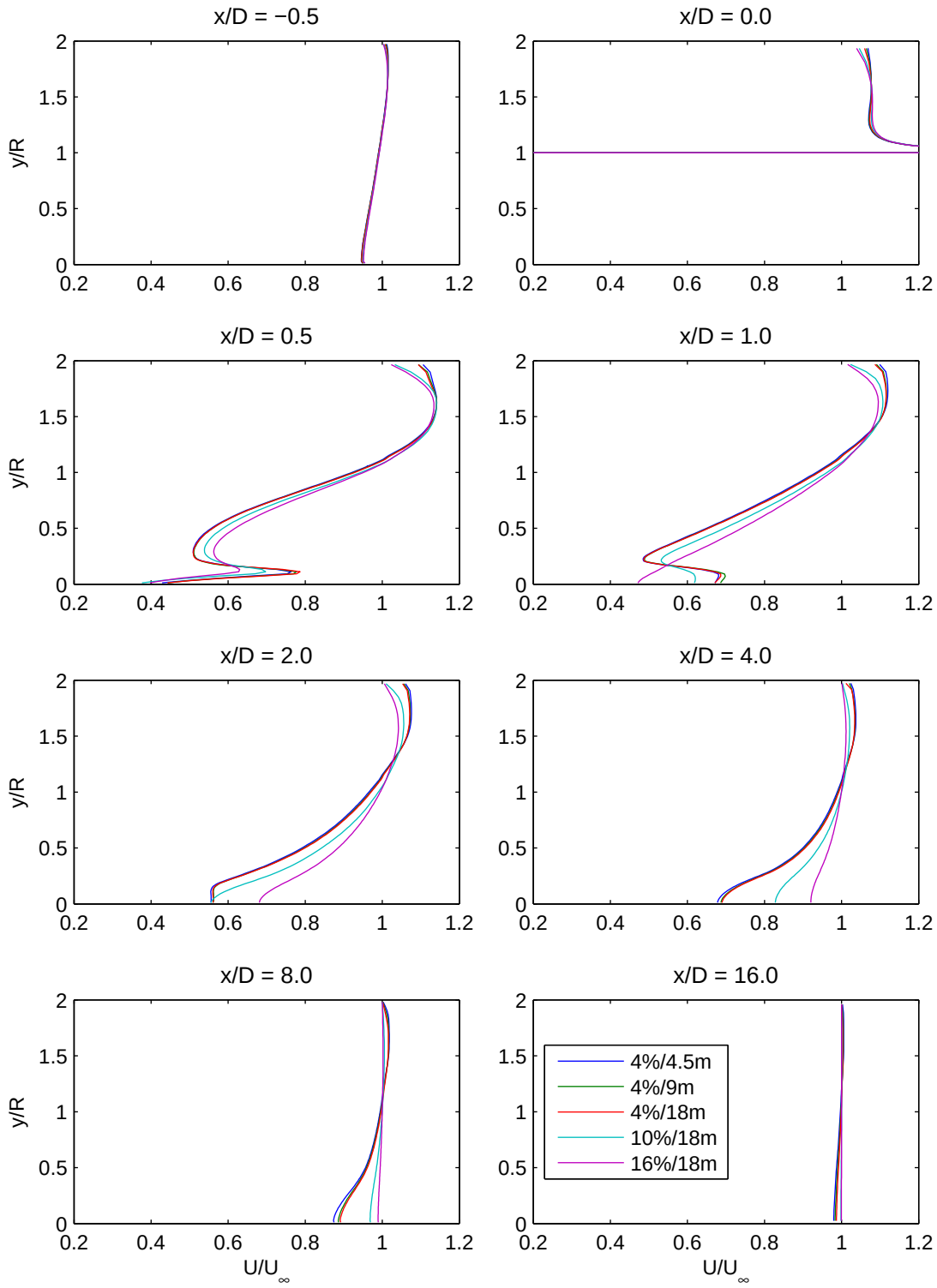

Figure 15: *Lateral velocity profiles.*

... low-solidity turbine, $R_d = 2R_t$, $\lambda = 5.0$

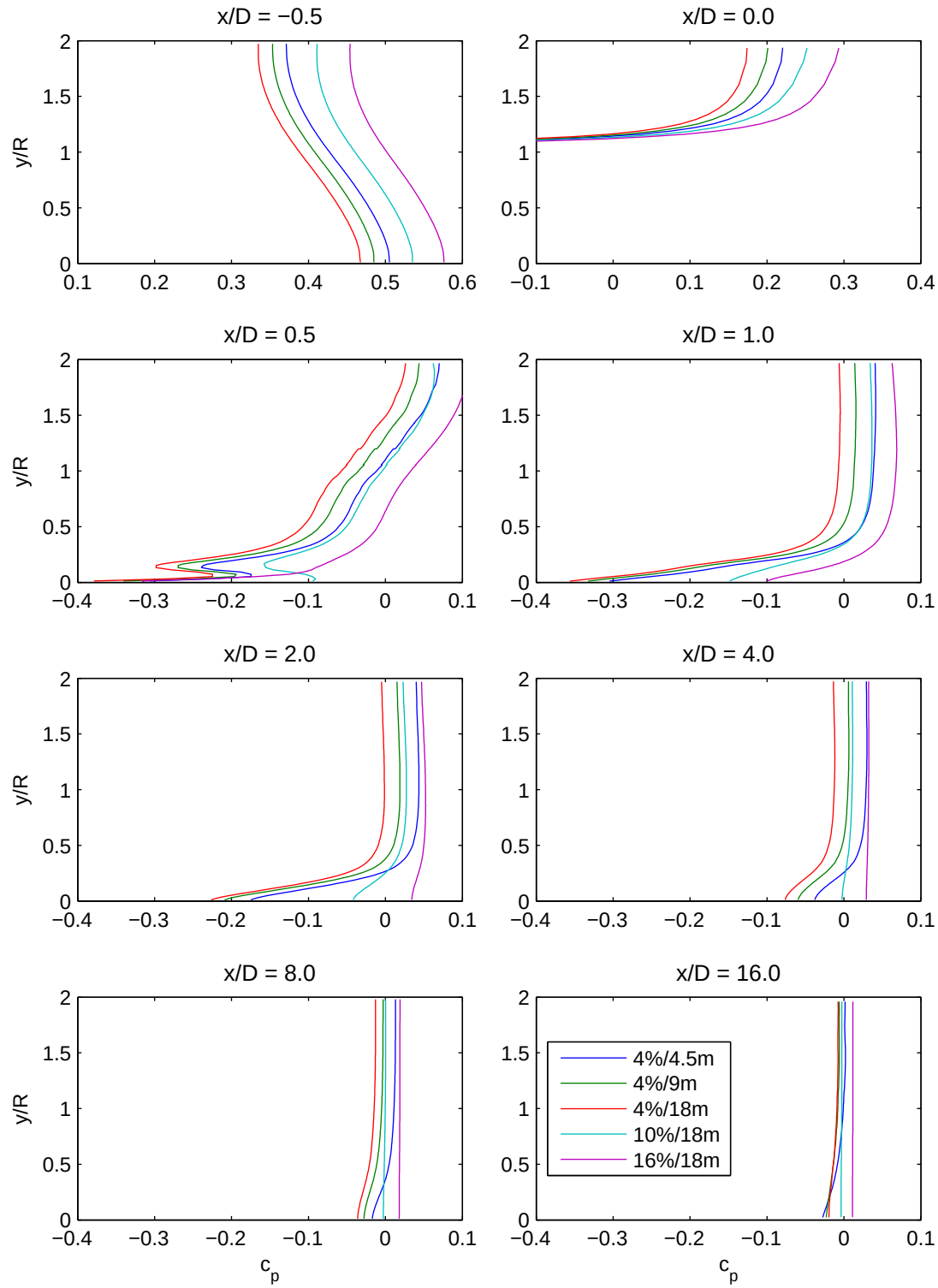

Figure 16: *Lateral pressure profiles.*

Low-solidity turbine, $R_d = 8R_t$**,** $\lambda = 5.0$

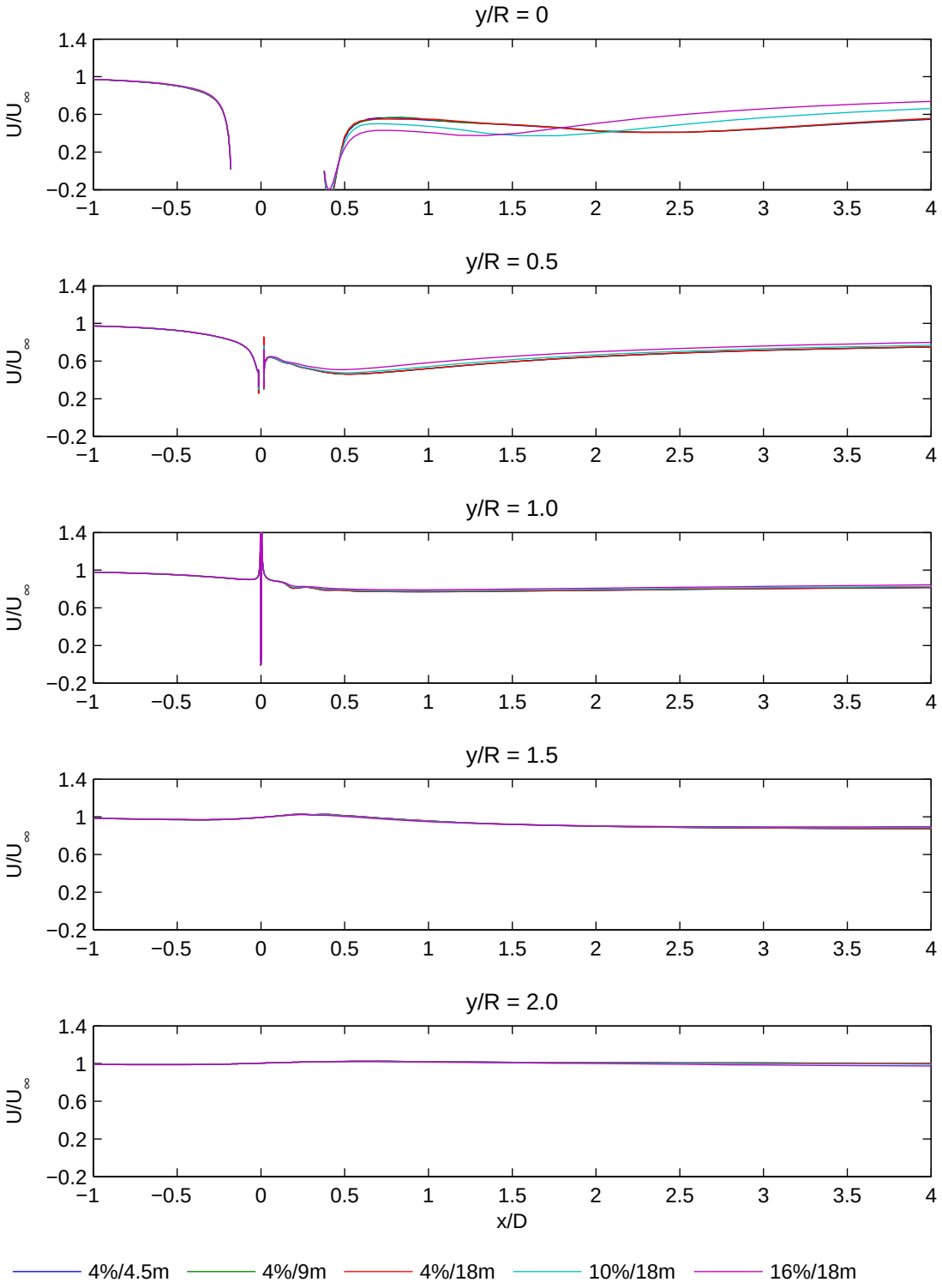

Figure 17: *Longitudinal velocity profiles.*

. . . low-solidity turbine, $R_d = 8R_t$, $\lambda = 5.0$ . . .

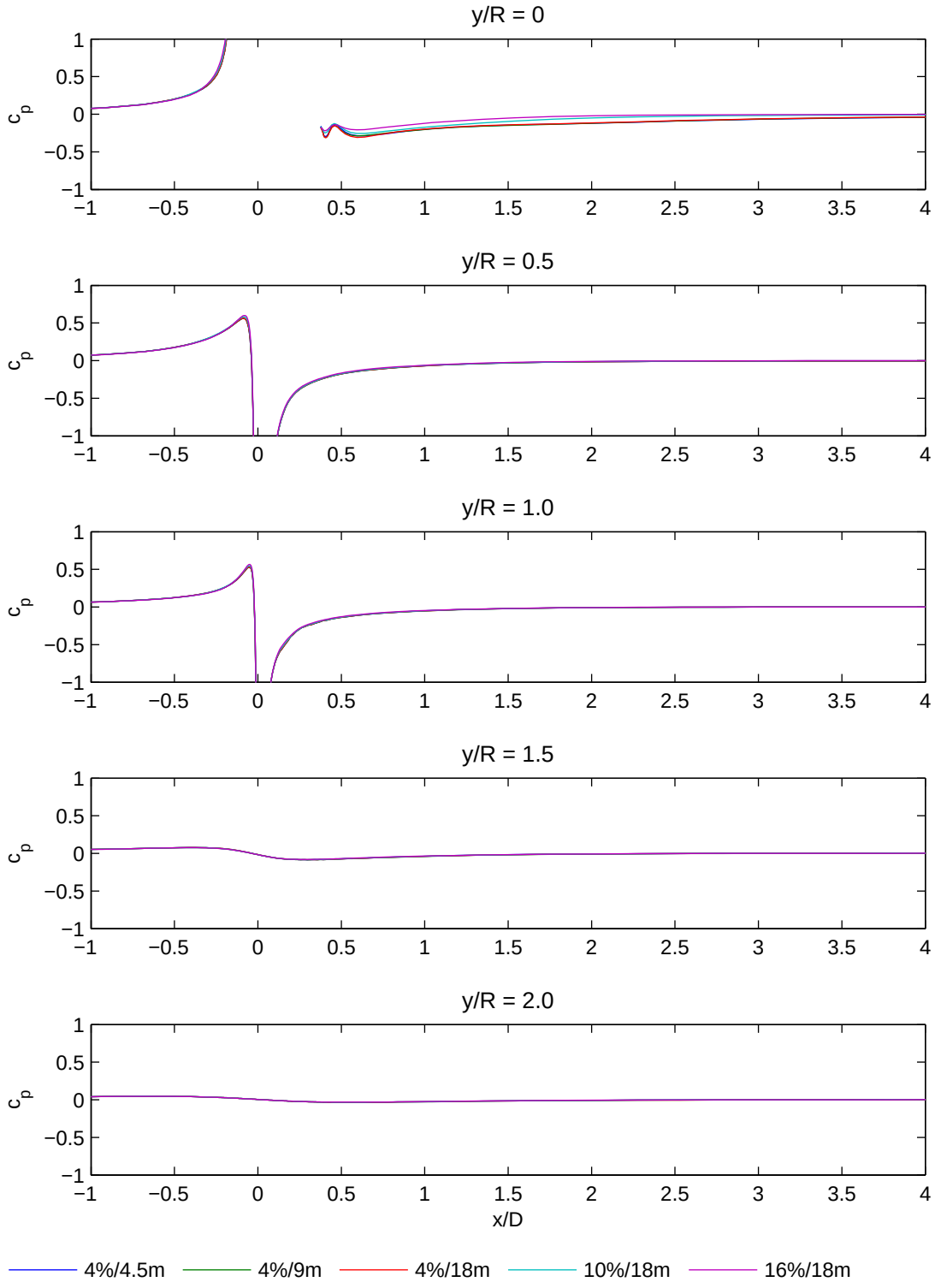

Figure 18: *Longitudinal pressure profiles.*

. . . low-solidity turbine, $R_d = 8R_t$, $\lambda = 5.0$ . . .

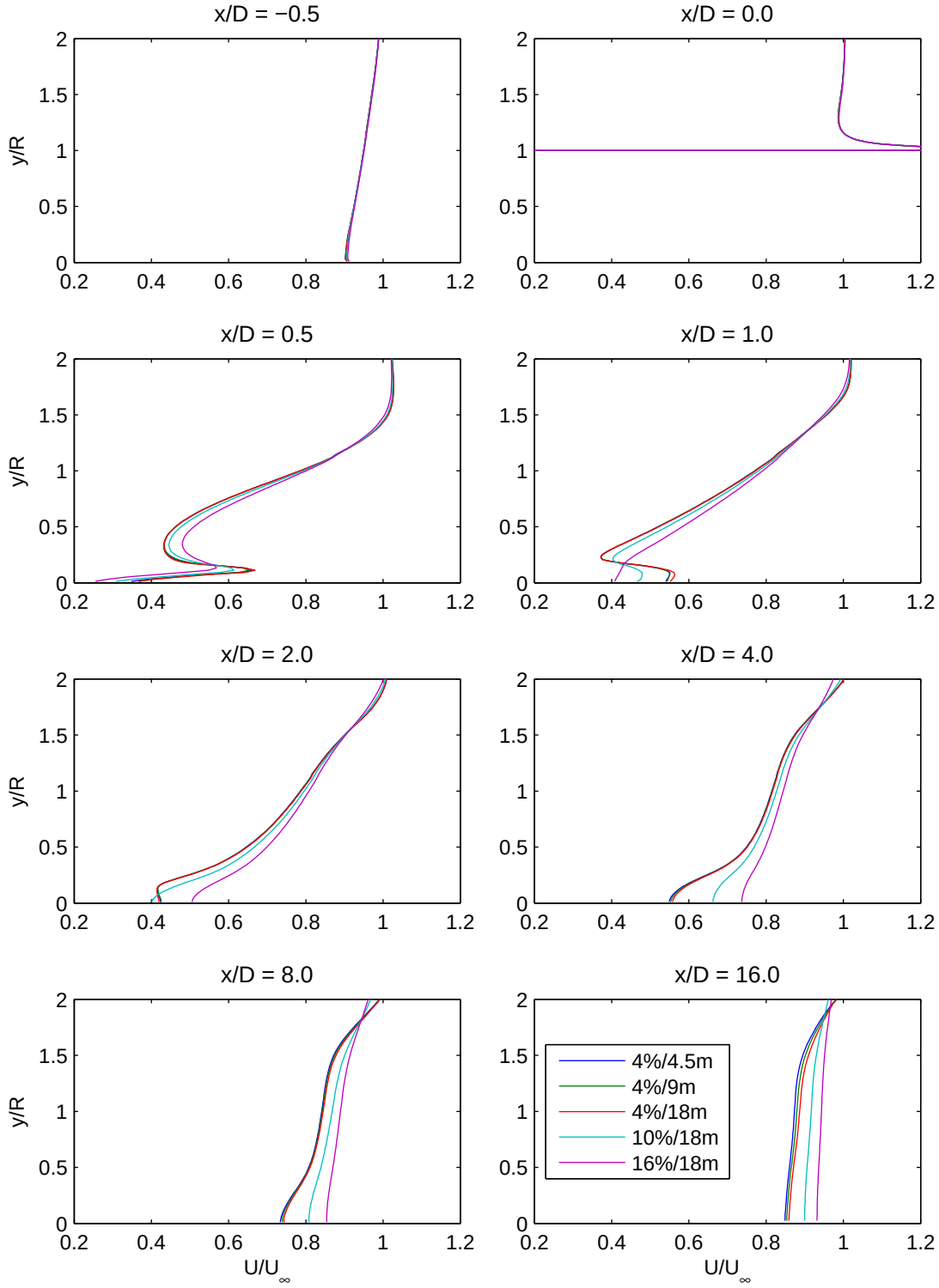

Figure 19: *Lateral velocity profiles.*

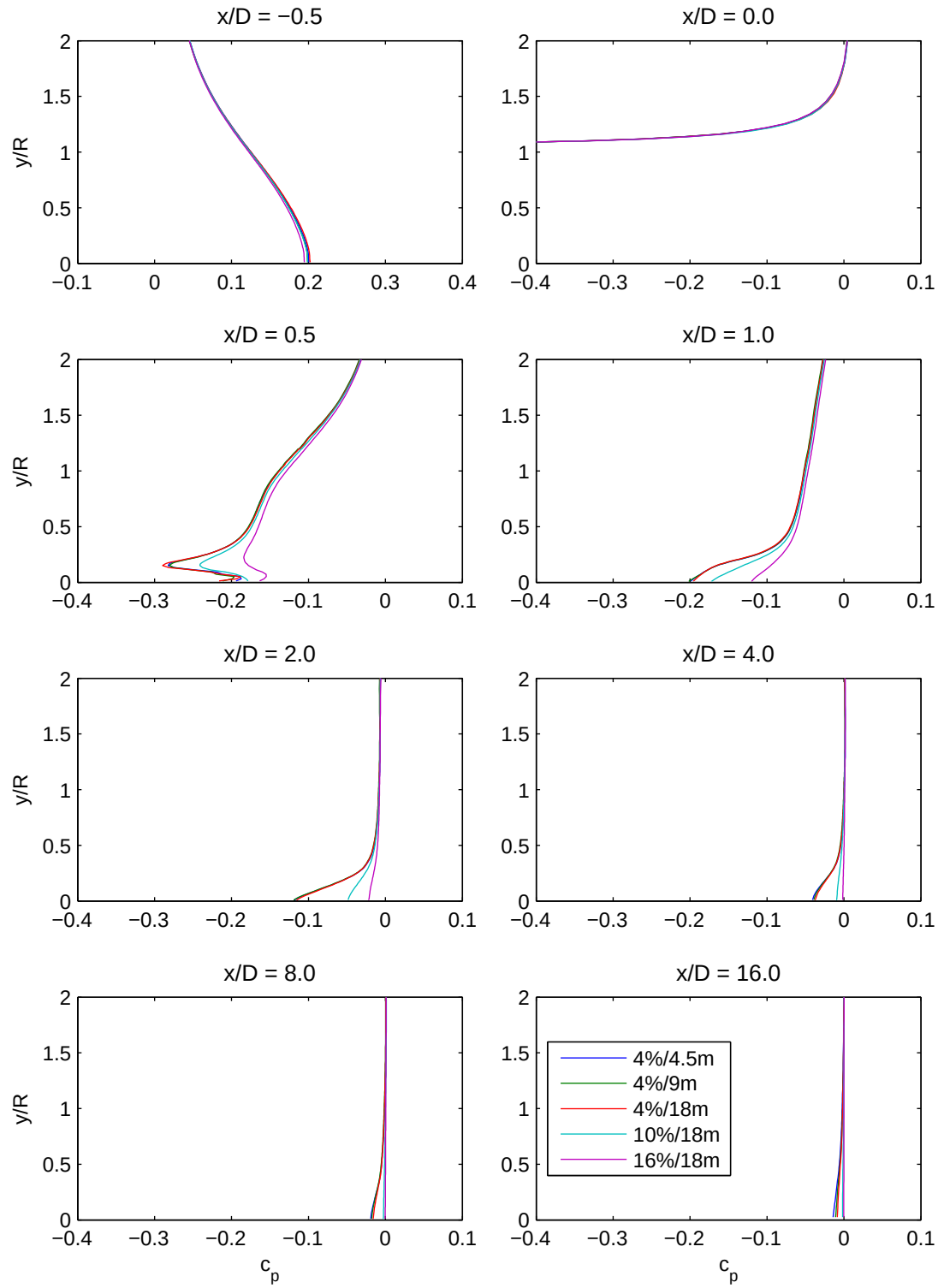

Figure 20: *Lateral pressure profiles.*

High-solidity turbine, $R_d = 4R_t$**,** $\lambda = 2.8$

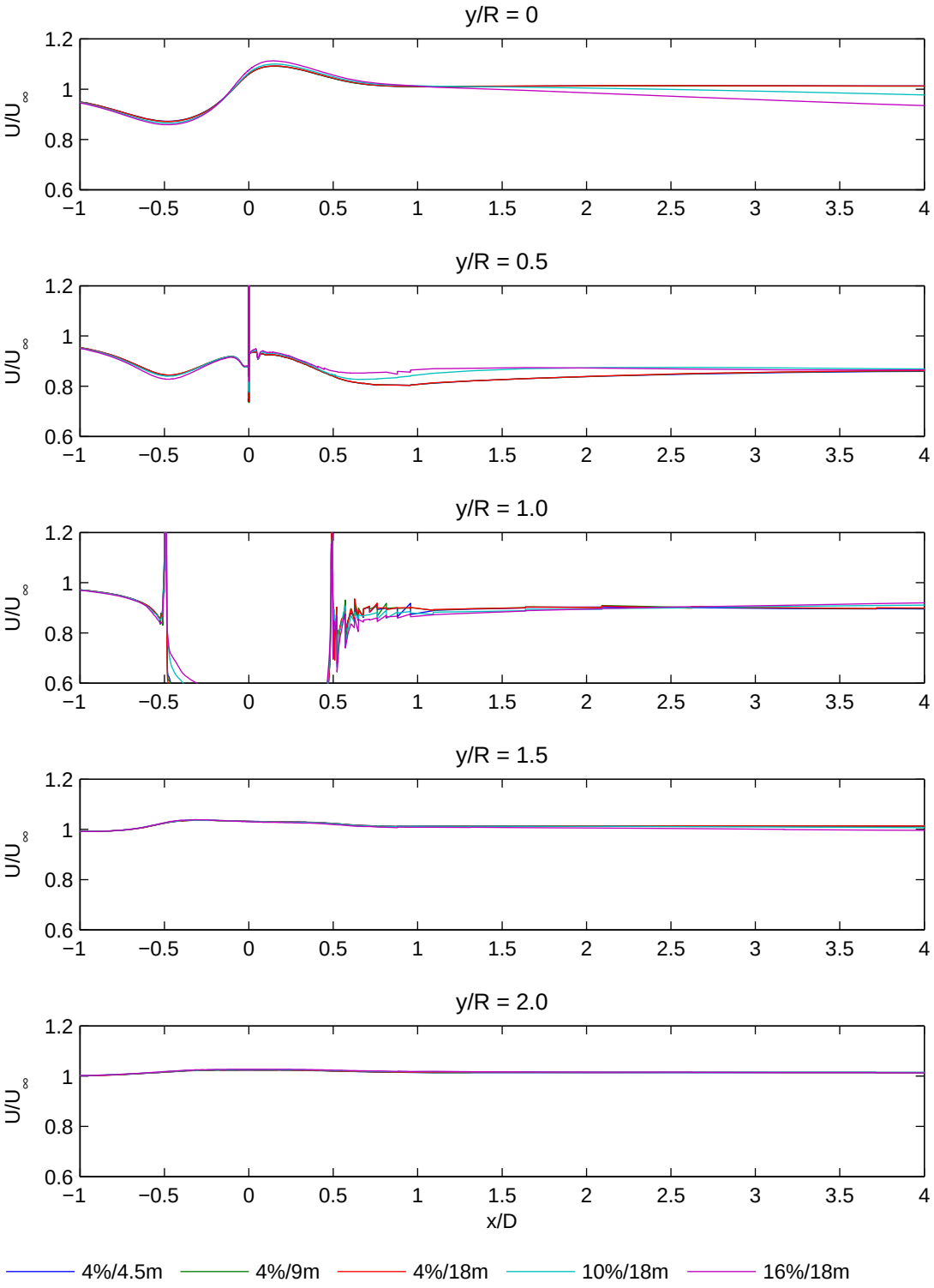

Figure 21: *Longitudinal velocity profiles.*

. . . high-solidity turbine, $R_d = 4R_t$, $\lambda = 2.8$ . . .

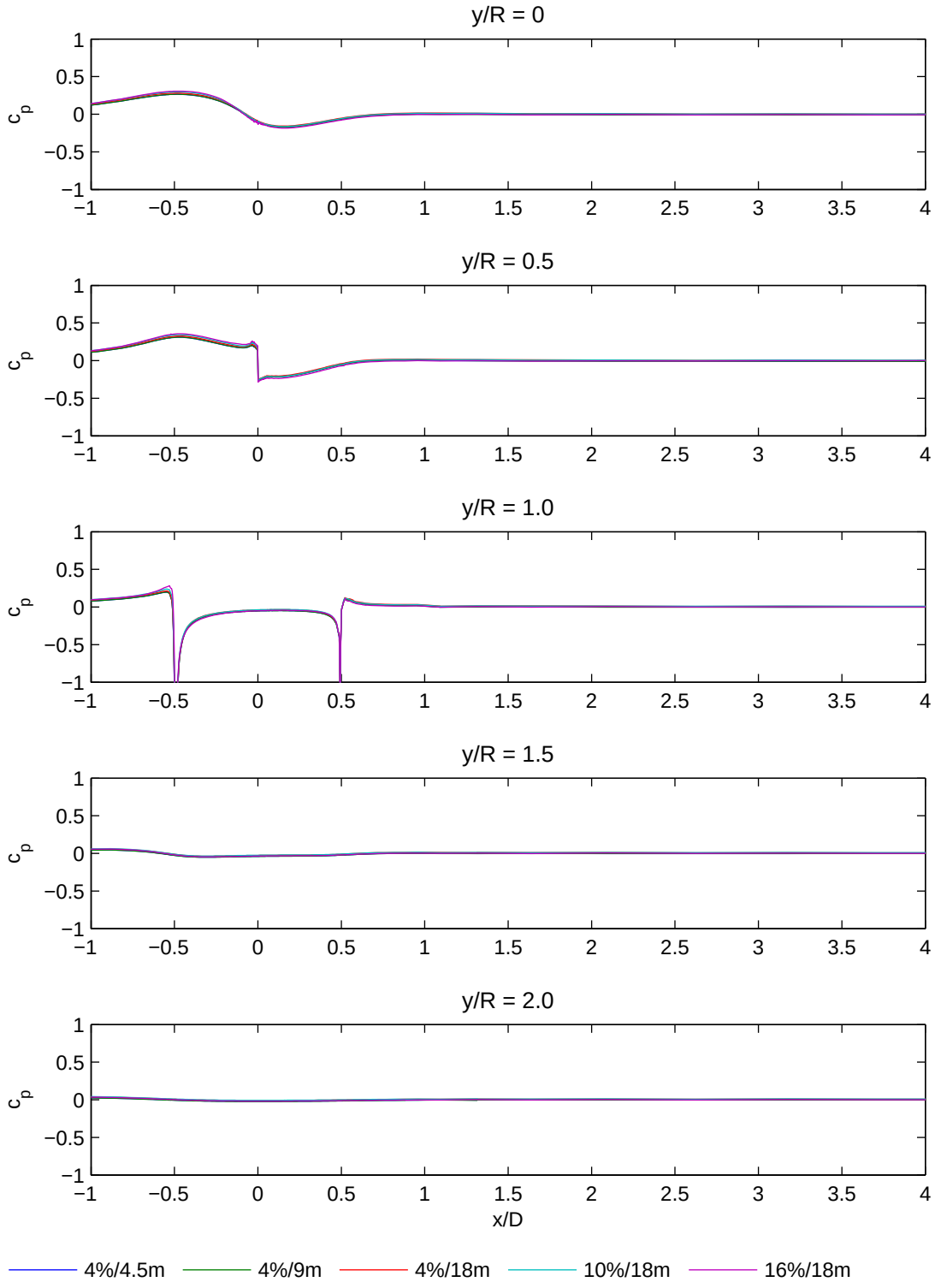

Figure 22: *Longitudinal pressure profiles.*

. . . high-solidity turbine, $R_d = 4R_t$, $\lambda = 2.8$ . . .

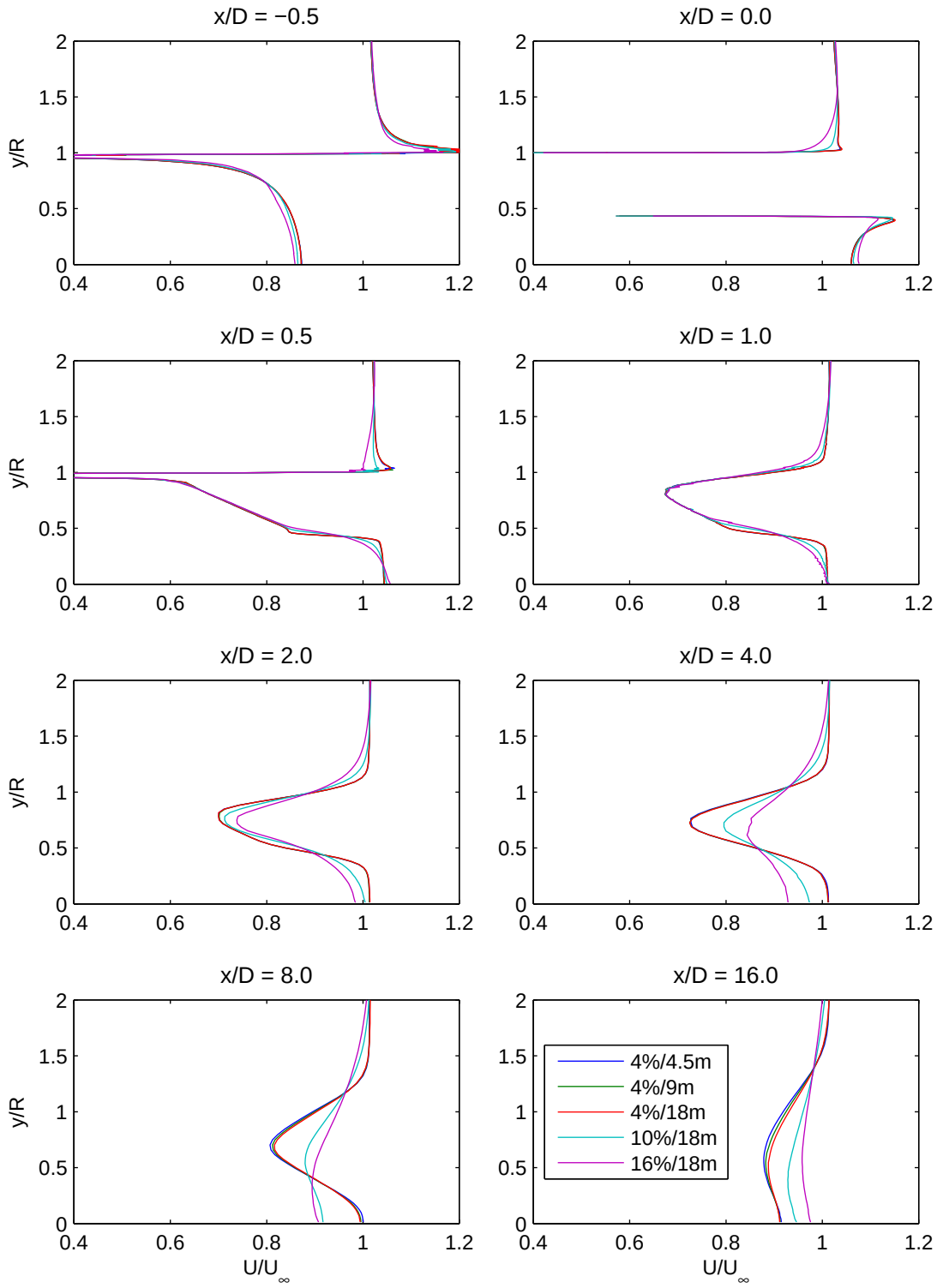

Figure 23: *Lateral velocity profiles.*

... high-solidity turbine, $R_d = 4R_t$, $\lambda = 2.8$

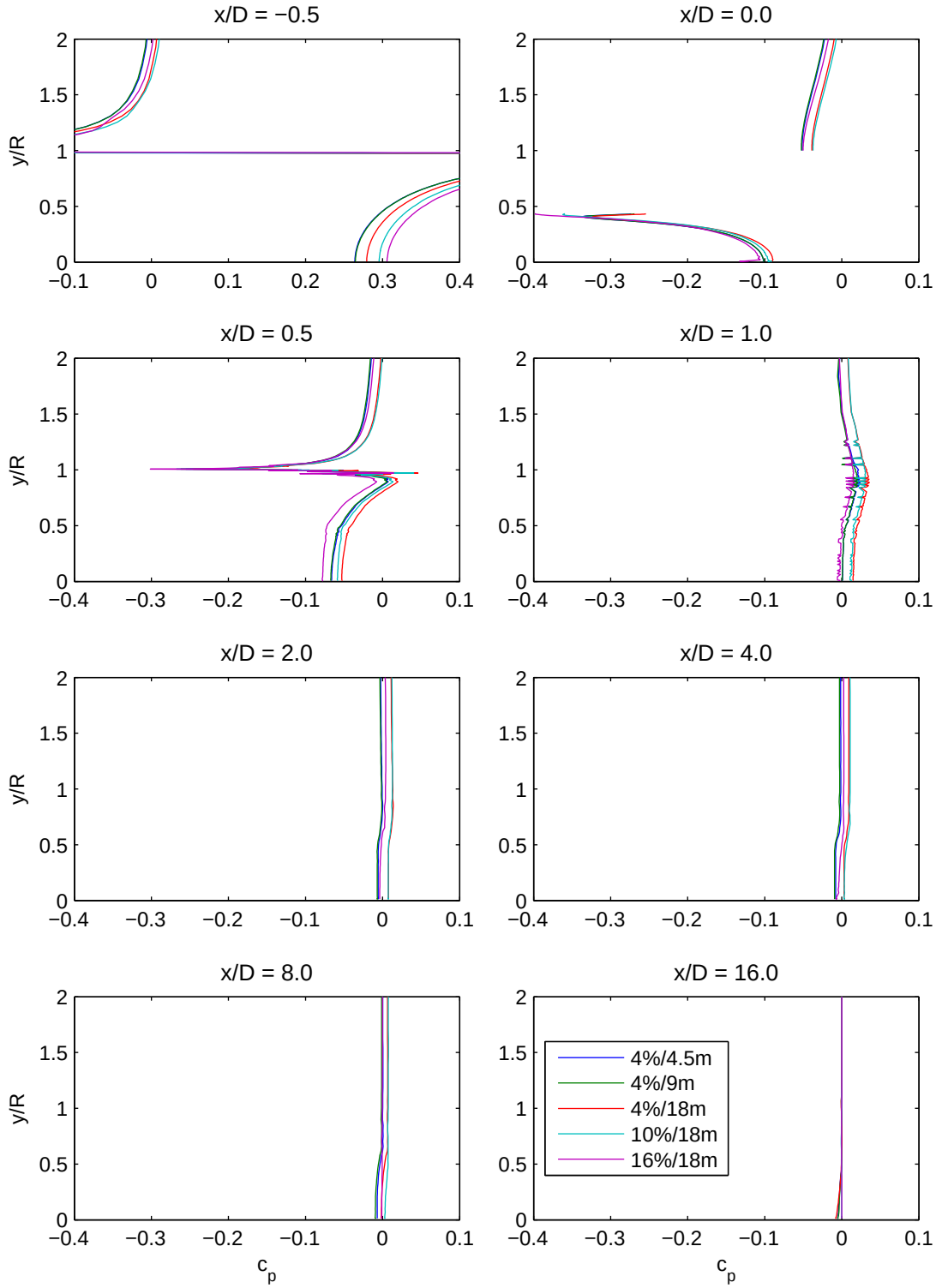

Figure 24: *Lateral pressure profiles.*

References

Gretton, G. I. (2011a), Development of a computational fluid dynamics model for a horizontal axis tidal current turbine – PerAWaT WG3 WP5 D1, Version 3.0, 12th December.

Gretton, G. I. (2011b), Development of a computational fluid dynamics model for an open-centre tidal current turbine – PerAWaT WG3 WP5 D2, Version 2.0, 9th December.

Gretton, G. I. (2013), A parameterization of the end-of-near-wake region for a conventional low solidity and an open-centre high-solidity tidal current turbine – PerAWaT WG3 WP5 D3, Version 1.0, 26th February.

Milne, I. A., Sharma, R. N., Flay, R. G. J., and Bickerton, S. (2011), Characteristics of the onset flow turbulence at a tidal-stream power site, in *Proceedings of the 9th European Wave and Tidal Energy Conference*, Southampton, UK.

Pope, S. B. (2008), *Turbulent Flows*, Cambridge University Press.

Versteeg, H. K. and Malalasekera, W. (2007), *An Introduction to Computational Fluid Dynamics: The Finite Volume Method*, Pearson, 2nd edition.